Evolution of pathogen traits in response to quantitative host resistance in heterogeneous environments

R. Djidjou-Demasse[a], S. Lion[b], A. Ducrot[c,d], J.-B. Burie[c,d], F. Fabre[a]

[a] *UMR 1065 SAVE, INRA, Bordeaux Sciences Agro, Villenave d'Ornon F-33882, France*

[b] *CEFE, CNRS, Univ. Montpellier, Univ. Montpellier 3 Paul-Valéry, EPHE, IRD, Montpellier F-34293, France*

[c] *Univ. Bordeaux, IMB, UMR 5251, F-33400 Talence, France*

[d] *CNRS, IMB, UMR 5251, F-33400 Talence, France.*

September 20, 2018

Abstract

Despite considerable studies on the adaptation of plant pathogens to qualitative resistance, few theoretical studies have investigated whether and how fast quantitative resistance can select for increased pathogen aggressiveness. In this paper, we formulate an integro-differential model with nonlocal mutation terms to describe the evolutionary epidemiology of fungal plant pathogens in heterogeneous agricultural environments. Parasites reproduce clonally and each strain is characterized by several phenotypic traits corresponding to the basic infection steps (infection efficiency, latent period, sporulation rate depending on the age of infection). We first derive a general expression of the basic reproduction number R_0 for fungal pathogens in heterogeneous environments, typically several cultivars cultivated in the same field (cultivar mixtures) or in different fields landscape (mosaics). Next, by characterizing the evolutionary endpoints of the coupled epidemiological evolutionary dynamics, we investigate how host heterogeneity and the effect of resistance on the pathogen traits impact the evolutionary dynamics of the pathogen population both at equilibrium and during transient epidemiological dynamics. We then show that the environmental feedback loop is one-dimensional and that the model admits an optimization principle relying on an R_0 maximization approach. We then highlight how one may take advantage of evolutionary dynamics leading to neutral coexistence to increase the durability of quantitative resistance, in particular for resistance genes targeting infection efficiency. Our analyses can guide experimentations by providing testable hypotheses and help plant breeders to design breeding programs.

Key words. Basic reproduction number; Evolutionary epidemiology;

Fungal pathogen; Quantitative resistance; Lifetime Reproduction success; Spore producing pathogens; Resistance durability.

1 Introduction

Resistance to parasites, i.e. the capacity of a host to decrease its parasite development (Raberg et *al.*, 2009; Restif & Koella , 2004), is a widespread defense mechanism in plants. Two types of resistance have been historically distinguished according to their phenotype: qualitative and quantitative resistances. Qualitative resistance usually confers disease immunity in such a way that parasites exhibit a discrete categorical distribution of their disease phenotype ("cause disease" versus "do not cause disease") (McDonald & Linde, 2002; St. Clair, 2010). By contrast, quantitative resistance leads to a reduction in disease severity (Poland et *al.*, 2009; St. Clair, 2010): parasites exhibit a continuous distribution of their disease phenotype (McDonald & Linde, 2002; St. Clair, 2010). Under quantitative resistance, all pathogen genotypes cause infection and reproduce, but they differ by their quantitative pathogenicity (*i.e.* aggressiveness) (Lannou, 2012; Zhan et *al.*, 2015). The inheritance of quantitative resistance most often relies on several genes, each contributing a small proportion of the resistance level (Pariaud et *al.*, 2009; Poland et *al.*, 2009; Lannou, 2012; Niks et *al.*, 2015). Among plant pathogens, fungal pathogens (*sensu lato, i.e.* including Oomycetes) are responsible for nearly one third of emerging plant diseases (Anderson et *al.* (2004)). Their pathogenicity is often estimated in laboratory experiments through a small number of quantitative pathogenicity traits (Pariaud et *al.*, 2009; Lannou, 2012) expressed during the basic steps of the host-pathogen interaction: (i) infection efficiency (probability that a spore deposited on a receptive host surface produces a lesion), (ii) latent period (time interval between infection and the onset of sporulation), (iii) sporulation rate (amount of spores produced per lesion and per unit time) and (iv) infectious period (time from the beginning to the end of sporulation). Quantitative resistance genes alter the expression of these pathogen life-cycle traits, sometimes through pleiotropic effects (*i.e.* effects on more than one trait (Parlevliet, 1986; Richardson et *al.*, 2006).

Plant resistance is often considered the most favorable method to manage plant diseases in agro-ecosystems for environmental, economic and social reasons (Mundt, 2014). Until now, plant breeders have mostly used qualitative resistances. Unfortunately this strategy leads frequently, and often rapidly, to resistance "breakdowns" caused by pathogen evolution (McDonald & Linde, 2002; Mundt, 2014; Zhan et *al.*, 2015). The most important argument for shifting from qualitative to quantitative resistances in cultivar breeding program is their supposed higher durability, resulting from their more complex genetic determinism (Niks et *al.*, 2015; Pilet-Nayel et *al.*, 2017). Nevertheless, both experimental evolution studies and field studies suggested that fungi and viruses adapt to quantitative resistance (see Pilet-Nayel et *al.* (2017) for a review). The resulting gradual "erosion" of the efficiency of quantitative resistance (McDonald &

Linde, 2002) corresponds to a gradual increase in quantitative pathogenicity. The polygenic inheritance of quantitative resistance suggests that multiple genetic changes will small effects are involved in the pathogen population. Without detailed knowledge of these genetic changes, fungi adaptation can be tracked in phenotype-fitness landscapes as proposed in Fisher's geometrical model (Fisher , 1930; Orr, 2005). The phenotype is represented by n pathogenicity traits and correlations between traits, observed for plant fungi (Pariaud et *al.*, 2009), can be taken into account (Martin & Lenormand, 2006). Mutations, produced by the successive asexual cycles occurring during the cropping season, randomly displace phenotypes in this n-dimensional space. They facilitate host local adaptation as they correspond, on a focal host, to as many cycles of selection for local adaptation without recombination breaking down *locally* advantageous allelic combinations (Giraud et *al.*, 2010).

Few theoretical studies have investigated whether and how fast quantitative resistance can select for increased pathogen aggressiveness in the field (Mundt, 2014). Predicting the dynamics of the erosion of quantitative resistances requires models coupling epidemiological and evolutionary dynamics in heterogeneous environment. Such models can be used to address the fundamental short- and long-term objectives of sustainable management of plant diseases (Zhan et *al.*, 2015): the short-term goal focuses on the reduction of disease incidence (epidemiology), whereas the longer-term objective is to reduce the rate of evolution of new pathotypes. In practice, this requires predictions on the transient evolutionary dynamics of pathogens, which can be formalised using the evolutionary epidemiology framework (Day & Proulx, 2004; Day & Gandon, 2006). Essentially inspired by quantitative genetics, it accounts for the interplay between epidemiological and evolutionary dynamics on the same time scale. It can be used to monitor the simultaneous dynamics of epidemics and dynamics of evolution of any set of pathogen life-history trait of interest. As far as we know, few studies (Iacono et *al.*, 2012; Papaïx et *al.*, 2018; Rimbaud et *al.*, 2018) applied the evolutionary epidemiology framework to study quantitative resistance erosion in agroecosystems. They showed that quantitative resistance that reduces the infection efficiency gives a greater yield benefit than quantitative resistance that reduces the sporulation rate. Moreover the evolutionary epidemiology framework can handle heterogeneous host populations resulting, for example, from differences in their genetic composition (Gandon & Day, 2007). Field mixtures, where several cultivars are cultivated in the same field, and landscapes mosaics, with cultivars cultivated in different fields, are a typical example. Host heterogeneity impacts parasite adaptive diversification and strain coexistence through complex spatial and temporal patterns of disruptive selection (Gandon , 2004; Barrett et *al.*, 2008; Metcalf et *al.*, 2015; David *al.*, 2017).

In this article, we follow this approach and study the evolutionary epidemiology of spore-producing pathogens in heterogeneous agricultural environments. In contrast with previous studies, we use an integro-differential model where the pathogen traits are represented as a vector of continuous traits, much like classically assumed in Fisher's geometrical model. This model extends previous

results of Djidjou-Demasse et *al.* (2017) to heterogeneous host populations where cultivars with quantitative resistances altering different pathogenicity traits are deployed. First, we investigate how heterogeneous environments differentially impact the pathogen population structure at equilibrium. This question is addressed by characterizing the evolutionary endpoints of the coupled epidemiological evolutionary dynamics. A particular emphasis will be put here on the differences between the cornerstone concepts of R_0 in epidemiology (Diekmann et *al.*, 1990; Van den Driessche & Watmough, 2008) and invasion fitness in evolution. Secondly we investigate how heterogeneous environments differentially impact the transient behavior of the coupled epidemiological evolutionary dynamics.

State variables	
$n_c \in \mathbb{N}^*$	Number of host classes.
$x \in \mathbb{R}^N$	"Label" on the pathogen strain.
$S_k(t)$	Density of healthy tissue of host k at time t.
$i_k(t,a,x)$	Density of infected tissue of host k at time t, which is infected since time a by pathogen strain x.
$A(t,x)$	Density of pathogen spores with strain x at time t.

Model parameters		
Parameters	Description	Unit
Λ	Influx of new healthy host tissue	HTD $\cdot$ Tu^{-1}
θ	Death rate of host tissue	Tu^{-1}
δ	Rate at which spore becomes unviable	Tu^{-1}
$d_k(a,x)$	Disease induced mortality of class k host tissue, infected by the pathogen strain x with age of infection a	Tu^{-1}
$\beta_k(x)$	Infection efficiency of the pathogen strain x on host k	SD^{-1} $\cdot$ Tu^{-1}
$p_k(x)$	Sporulation rate of the pathogen strain x on host k	SD $\cdot$ HTD^{-1} $\cdot$ Tu^{-1}
$\tau_k(x)$	Latent period of the pathogen strain x on host k	Tu
$l_k(x)$	Infectious period of the pathogen strain x on host k	Tu
φ_k	Proportion of host class k at the disease free equilibrium	unitless
ε	Distance beyond which non-local mutations become "negligible"	unitless
$m_\varepsilon(x-y)$	Mutation probability from pathogen strain x to y	unitless

Tu= time unit; SD= spores density; HTD=host tissue density

Table 1: Description of the state variables and parameters of the model.

2 A structured model of epidemiological and evolutionary dynamics

2.1 Host and pathogen populations

We consider an heterogeneous host population with $n_c \in \mathbb{N}^*$ host classes infected by a polymorphic spore-producing pathogen population. Here, host heterogeneity may refer to different host classes, but also to different host developmental

stages, sexes, or habitats. The host population is further subdivided into two compartments: susceptible or healthy host tissue (S) and infectious tissue (I). In keeping with the biology of fungal pathogens, we do not track individual plants, but rather leaf area densities (leaf surface area per m^2). The leaf surface is viewed as a set of individual patches corresponding to a restricted host surface area that can be colonized by a single pathogen individual. Thus only indirect competition between pathogens strains for a shared resource is considered.

The parasite is assumed to reproduce clonally and to produce spores. Spores produced by all infectious tissues are assumed to mix uniformly in the air and then land on any host class according to the law of mass action, that is the probability of contact between a spore and host k is proportional to the total susceptible leaf surface area of this host. In the model, the density of airborne spores is denoted by A. Each strain of the pathogen population is further characterised by four phenotypic pathogenicity traits, corresponding to the 4 basic steps of the disease infection cycle : (i) infection efficiency (probability that a spore deposited on a receptive host surface produces a lesion), (ii) latent period (time interval between infection and the onset of sporulation), (iii) sporulation rate (number of spores produced per lesion and per unit time) and (iv) infectious period (time from the beginning to the end of sporulation). The model also takes into account mutations. Mutations are modeled with a multivariate distribution m representing the random displacement in the phenotypic space at each generation.

2.2 Model

We introduce a set of integro-differential equations modeling the epidemiological and the evolutionary dynamics of spore-producing pathogens in a heterogeneous host population. Table 1 lists the state variables and parameters of the model. A key feature of our model is that we explicitly track both the age of infection in infected hosts and the pathogen strain. This leads to the following non-local age-structured system of equations posed for time $t > 0$, age since infection $a > 0$ and phenotypic value $x \in \mathbb{R}^N$, for some integer $N \geq 1$ (the dimension of the pathogen phenotypic space),

$$\begin{cases} \partial_t S_k(t) = \varphi_k \Lambda - \theta S_k(t) - S_k(t) \displaystyle\int_{\mathbb{R}^N} \beta_k(y) A(t,y) \mathrm{d}y, \\ (\partial_t + \partial_a)\, i_k(t,a,x) = -\left(\theta + d_k(a,x)\right) i_k(t,a,x), \\ i_k(t,0,x) = \beta_k(x) S_k(t) A(t,x), \\ \partial_t A(t,x) = -\delta A(t,x) + \displaystyle\sum_{l=1}^{n_c} \int_{\mathbb{R}^N} \int_0^\infty m_\varepsilon(x-y) r_l(a,y) i_l(t,a,y) \mathrm{d}a \mathrm{d}y. \end{cases} \tag{2.1}$$

Model (2.1) considers n_c host classes. $S_k(t)$ is the density of healthy tissue in class k at time t, $i_k(t,a,x)$ the density of tissue in class k that was infected at time $t-a$ by a pathogen with phenotypic value x, and $A(t,x)$ denotes the density of spores with phenotypic value x at time t. Without disease, susceptible hosts

are produced at rate $\Lambda > 0$ and die at rate $\theta > 0$, regardless of their class. φ_k is the proportion of the host class k at the disease free equilibrium. In presence of the disease, susceptible hosts can become infected by airbone spores. The total force of infection on a host in class k is $h_k(t) = \int \beta_k(y)A(t,y)\mathrm{d}y$. Infected hosts die at rate $\theta + d_k(a,x)$ where $d_k(a,x)$ is the disease-induced mortality of infected tissue with age of infection a. Airborne spores produced by infected hosts become unviable at rate $\delta > 0$. Hosts infected by strain y produce airborne spores with phenotype x at a rate $m_\varepsilon(x-y)r_k(a,y)$, where $m_\varepsilon(x-y)$ is the probability of mutation from phenotype y to phenotype x and $r_k(a,y)$ is the sporulation function, which depends on host class, age of infection and the phenotype of the parasite.

The age-specific sporulation function $r_k = r_k(a,x)$ can take several forms (Figure 1 A) Segarra et *al.* (2001). For instance, a block function assumes that during the infectious period, a lesion produces a constant number of spores per unit of time:

$$r_k(a,x) = \begin{cases} p_k(x) & \text{if } \tau_k(x) \leq a \leq \tau_k(x) + l_k(x), \\ 0 & \text{otherwise,} \end{cases} \tag{2.2}$$

where p_k, τ_k and l_k denote the strain-specific sporulation rate, latent period and infectious period in the k-class respectively. Alternatively, a gamma distribution with parameters $\lambda > 0$ and $n > 0$ can be used:

$$r_k(a,x) = \begin{cases} p_k(x)l_k(x)\frac{\lambda^n(a-\tau_k(x))^{n-1}\exp[-\lambda(a-\tau_k(x))]}{\Gamma(n)} & \text{if } a \geq \tau_k(x), \\ 0 & \text{otherwise.} \end{cases} \tag{2.3}$$

The kernel m_ε represents the effects of mutations that randomly displace phenotypes at each generation. To fix ideas, a multivariate Gaussian distribution $m = N(0,\Sigma)$ leads to $m_\varepsilon(x-y) = \frac{1}{\varepsilon^N} m\left(\frac{x-y}{\varepsilon}\right)$. The covariance terms of Σ allow to take into account trade-offs between the pathogen life-history traits both within- and between host-classes. They emerge from the mutation process (Gandon , 2004). The mutation kernel m is not restricted to Gaussian distributions, provided it satisfies some properties such as positivity and symmetry (Appendix B). Finally, note that the formulation of model (2.1) encompasses several models of the literature (Appendix C).

3 Basic reproduction number in disease-free and infected environment

3.1 Basic reproduction number

The basic reproduction number (usually denoted $\mathcal{R}_0$) is defined as the total number of infections arising from one newly infected individual introduced into a healthy (disease-free) host population (Diekmann et *al.*, 1990; Anderson, 1991). The disease free equilibrium density of susceptible hosts in class k is $S_k^0 = \varphi_k\Lambda/\theta$. A pathogen with phenotype x will spread if his basic reproduction number in

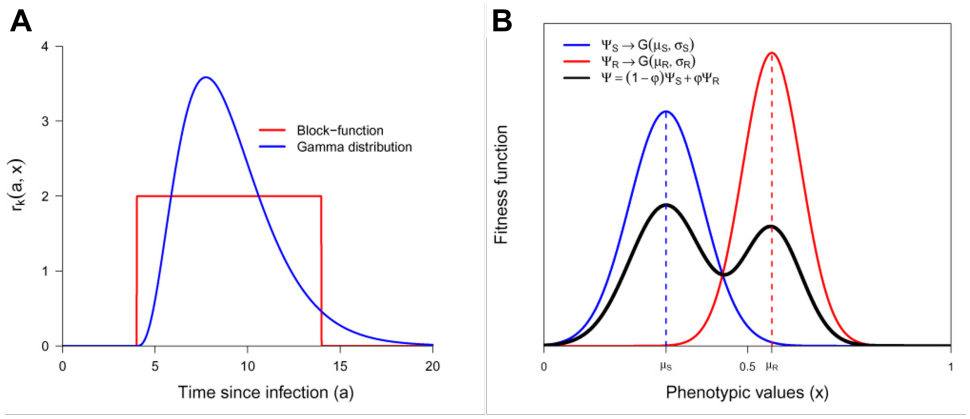

Figure 1: **A** Possible shapes of sporulation curves. Amount of spores produced, $r_k(a, x)$, by an infected tissue which is infected since time a. For the gamma shape (equation (2.3)), the parameters are the latent period ($\tau_k = 4$), the sporulation rate ($p_k = 8$), the infectious period ($l_k = 10$), $n = 8$ and $\lambda = 0.8$. For the block-function shape (equation (2.2)), the parameters τ_k and l_k are the same as for the gamma distribution. The sporulation rate $p_k \approx 1.997$ was chosen such that the area under both curves are the same. **B** An adaptive landscape with two local fitness peaks in a dual host environment. The fitness function Ψ of the pathogen population is described by a Gaussian mixture model: $\Psi = (1-\varphi)G(\mu_S, \sigma_S) + \varphi G(\mu_R, \sigma_R)$, wherein $G(\mu_k, \sigma_k)$ states for the Gaussian function with expected value μ_k and variance σ_k^2. For the k-host class, μ_k is the optimal phenotypic value while $1/\sigma_k^2$ is its selectivity. φ, the proportion of R host in the environment, is the mixture parameter.

the environment composed with n_c host classes is such that $\mathcal{R}_0(x) > 1$, and where

$$\mathcal{R}_0(x) = \sum_{k=1}^{n_c} \mathcal{R}_0^k(x), \tag{3.4}$$

wherein $\mathcal{R}_0^k(x)$ is the basic reproduction number of a pathogen with phenotype x in the k-host environment defined by $\mathcal{R}_0^k(x) = \frac{\Lambda}{\theta}\varphi_k \Psi_k(x)$, and $\Psi_k(x)$ is given by

$$\Psi_k(x) = \frac{1}{\delta}\beta_k(x) \int_0^\infty r_k(a,x) \exp\left(-\theta a - \int_0^a d_k(\sigma,x)\mathrm{d}\sigma\right) \mathrm{d}a, \tag{3.5}$$

for all $k \in \{1, \ldots, n_c\}$. The function $\Psi_k(x)$ has an immediate interpretation as the total effective number of spores with phenotype x landing on host class k and triggering an infection (see Appendix D for details on calculations).

If d_k doesn't depend on the age of infection, Ψ_k can be simplified. In particular, with a block function sporulation curve r_k, we obtained

$$\Psi_k(x) = \frac{1}{\delta} \cdot \frac{1}{\theta + d_k(x)} \cdot \beta_k(x) \cdot p_k(x) \cdot e^{-(\theta + d_k(x))\tau_k(x)} \cdot \left[1 - e^{-(\theta + d_k(x))l_k(x)}\right], \tag{3.6}$$

With a gamma shape sporulation curve r_k, we obtained

$$\Psi_k(x) = \frac{1}{\delta} \cdot \frac{l_k(x)}{\left[1 + (\theta + d_k(x))/\lambda\right]^n} \cdot \beta_k(x) \cdot p_k(x) \cdot e^{-(\theta + d_k(x))\tau_k(x)}. \tag{3.7}$$

Terms in equation $\Psi_k(x)$ represent (i) the life time of an offspring, $1/\delta$, (ii) the infection duration, $1/(\theta + d_k(x))$ or $l_k(x)/\left[1 + (\theta + d_k(x))/\lambda\right]^n$, (iii) the probability that an infected host dies before infection ends (as opposed to recovering), $(1 - e^{-(\theta + d_k(x))l_k(x)})$ and (iv) the probability for an infected host to survive the latent period, $e^{-(\theta + d_k(x))\tau(x)}$. If furthermore r_k is independent of a, we recover the classical expression of $\mathcal{R}_0$ for SIR models (see e.g. Day (2002))

$$\mathcal{R}_0(x) = \frac{\Lambda}{\theta} \sum_{k=1}^{n_c} \varphi_k \frac{\beta_k(x) r_k(x)}{\delta(\theta + \mathrm{d}_k(x))}. \tag{3.8}$$

3.2 Lifetime reproduction success and its proxy

$\mathcal{R}_0$ applies to study the spread of a pathogen strain x in an *uninfected* host population. To study the spread of a new mutant strain in a host population *already infected* by a resident strain x, we can use the adaptive dynamics methodology to calculate the invasion fitness (Dieckmann, 2002; Diekmann et *al.*, 2005; Geritz et *al.*, 1997; Metz et *al.*, 1996). Here, we work in generation time and use the lifetime reproductive success of a rare mutant as a fitness proxy. Once the pathogen spreads, let us assume that the population reaches a monomorphic endemic equilibrium denoted by $E^x = (S_k^x, i_k^x(\cdot), A^x)_{k=1,\cdots n_c}$,

for some trait x. Note that E^x is the environmental feedback of the resident x. Calculations are detailed in Appendix D along with the expression of S_k^x, $i_k^x(\cdot)$ and A^x. A rare mutant with phenotype y will invade the resident population infected by the strain x if $\mathcal{R}(x,y) > 1$, where

$$\mathcal{R}(x,y) = \sum_{k=1}^{n_c} S_k^x \Psi_k(y). \tag{3.9}$$

Expressions for $\mathcal{R}(x,y)$ and $\mathcal{R}_0(x)$ have a strong analogy. Both expressions are basic reproduction ratios that measure the weighted contribution of the pathogen to the subsequent generations, but while $\mathcal{R}_0(x)$ is calculated in the disease-free environment $E^0 = \left(S_1^0, \ldots, S_{n_c}^0, 0, \ldots, 0\right)$, $\mathcal{R}(x,y)$ is calculated in the environment set by the resident strain E^x. Note that the equation defining the endemic equilibrium ((D.7) in Appendix D) is simply the resident equilibrium condition $\mathcal{R}(x,x) = 1$.

$\mathcal{R}(x,y)$ takes the form of a sum of the mutant pathogen's reproductive success in each host class. In a two-class model, Gandon (2004) showed that this is not generally true, unless between-class transmission can be written as the product of host susceptibility times pathogen transmissibility. This is equivalent to the more general statement that pathogen propagules all pass through a common pool, as in our model in the compartment $A(.)$ (see Rueffler & Metz (2013) for a general treatment).

3.3 $\mathcal{R}_0$ maximization and the optimization principle

When infection efficiencies do not differ between host classes (i.e. $\beta_k(x) = \beta(x)$ $\forall\, k$), the fitness proxy $\mathcal{R}(x,y)$ can be written as $\mathcal{R}(x,y) = \frac{\Lambda}{\theta+\beta(x)A^x}\Psi(y) = \frac{\Psi(y)}{\Psi(x)}$, where

$$\Psi(x) = \sum_{k=1}^{n_c} \varphi_k \Psi_k(x). \tag{3.10}$$

The equality $\mathcal{R}(x,y) = \Psi(y)/\Psi(x)$ is obtained from the equation (D.7) in Appendix D defining the endemic equilibrium. It follows that a rare mutant will invade the population if $\Psi(y) > \Psi(x)$ or $\mathcal{R}_0(y) > \mathcal{R}_0(x)$, which simply means that pathogen evolution leads to R_0 maximisation. In this case, we can use R_0 or Ψ as a measure of absolute fitness. However this is not a general property of host-pathogen systems (see e.g. Lion & Metz (2018) for a more general discussion). In particular, when infection efficiencies differ between host classes, $\mathcal{R}$ rather than R_0 or Ψ must be used as the fitness proxy (Appendix E).

4 Effect of life-cycle components on the evolutionary dynamics

In this section, drawing on an agricultural example, we firstly characterize the evolutionary endpoints of the coupled epidemiological and evolutionary dynamics described by model (2.1) using the shape of the fitness function Ψ. Then we

study how the population reaches this equilibrium state through a mutation-selection process and highlight how these transient dynamics inform management strategies.

4.1 Case-study : deployment of a plant resistant cultivar

We consider a monomorphic plant pathogen population resulting from the monoculture of a single plant cultivar, called susceptible (S), during a long-time. A new cultivar bearing a quantitative resistance gene, called resistant (R), is introduced at $t = 0$ in a proportion φ of the environment.

We assume that the quantitative resistance gene alters a single pathogenicity trait, characterized in both cultivars, by normally distributed values. This leads to Gaussian fitness functions $\Psi_k \hookrightarrow G(\mu_k, \sigma_k^2)$ where μ_k is the optimal phenotypic value on the host k and $1/\sigma_k^2$ is the host selectivity (Papaïx et *al.*, 2013). With two host classes, $\Psi = (1-\varphi)\Psi_S + \varphi\Psi_R$ is a Gaussian mixture with 5 parameters (Figure 1). We assume that the R cultivar is less selective than the S cultivar ($\sigma_S \leq \sigma_R$). The trade-off $\rho_{S,R} = |\mu_S - \mu_R|/(\sqrt{2(\sigma_S^2 + \sigma_R^2)})$ measures to what extent the adaptation to the R cultivar causes maladaptation to the S cultivar (Papaïx et *al.*, 2013; Débarre & Gandon, 2010). It is closely linked to the competitive overlap between S and R hosts (Macarthur & Levins, 1967). If $\rho_{S,R} < 1$, Ψ has a unique maximum and the trade-off is weak (Behboodian, 1970). If $\rho_{S,R} > 1$, Ψ has two local maxima and the trade-off is strong.

We design simulations to analyze how the choices of (i) the pathogenicity trait targeted by the R gene, (ii) the level of resistance effectiveness (as measured by the adaptation trade-off $\rho_{S,R}$) and (iii) the deployment strategy (proportion φ of fields sown with the R cultivar) affect the durability of the R cultivar. The durability was quantified by T_{inf}, the time when at least 5% of the leaf area density of the R cultivar is infected (*i.e.* time t from which the following inequality is always satisfied $\int I_R(t,x)\mathrm{d}x / \left(S_R(t) + \int I_R(t,x)\mathrm{d}x\right) \geq 5\%$). T_{inf} characterize the time of the beginning of erosion of the R cultivar. Additionally, we assessed T_{shift}, the time when at least 50% of the pathogen population infecting the R cultivar belongs to adapted strains (*i.e.* time t from which the following inequality is always satisfied $I_R(t,\mu_R)/\left(I_R(t,\mu_S) + I_R(t,\mu_R)\right) \geq 50\%$). Finally,we assessed the epidemiological protection provided by the deployment of the R cultivar using the relative Healthy Area Duration (HAD) gain. Following Iacono et *al.* (2012), we defined relative HAD $= \frac{\int_0^{T\max}(S_S+S_R)(t)|_\varphi \mathrm{d}t}{\int_0^{T\max}(S_S(t))|_{\varphi=0}\mathrm{d}t}$.

Parameters used for simulations are given in Table 2. Initially, we set $S_S(0) = (1-\varphi)\frac{\Lambda}{\theta}$, $S_R(0) = \varphi\frac{\Lambda}{\theta}$, $I_S(0,x) = G(\mu_S, \sigma_S/2)(x)$ and $I_R(0,x) = 0$. Simulations were sped up using a simplified model, without age structure and by assuming that the evolution of the density of airborne spores is a fast process (*i.e.* the density of airborne spores reach rapidly an equilibrium, $\partial_t A(t,x) \equiv 0$,

compared to the host dynamics). It reads

$$\begin{cases} \partial_t S_k(t) = \varphi_k \Lambda - \theta S_k(t) - S_k(t) \displaystyle\int_{\mathbb{R}^N} \beta_k(y) A(t,y) \mathrm{d}y, \\ \partial_t I_k(t,x) = \beta_k(x) S_k(t) A(t,x) - (\theta + d_k(x))\, I_k(t,x), \\ \text{with} \\ A(t,x) = \dfrac{1}{\delta} \displaystyle\sum_{l=1}^{n_c} \int_{\mathbb{R}^N} m_\varepsilon(x-y) p_l(y) I_l(t,y) \mathrm{d}y. \end{cases} \tag{4.11}$$

	Fixed parameters	
ε	Distance beyond which non-local mutations become "negligible"	0.05
$m_\varepsilon(x-y)$	Probability that a pathogen strain x mutates to y	$G(0,\varepsilon)$
Λ	Influx of new healthy host tissue	35
θ	Death rate of host tissue	1
δ	Rate at which spore becomes unviable	1
$d_S(a,x)$, $d_R(a,x)$	Disease induced mortality of S and R cultivars	0
μ_S	The optimal phenotypic value on the S cultivar	0.3
$1/\sigma_S^2$	The selectivity of S cultivar	$(1/0.06)^2$
	Studied parameters	
φ	Proportion of the R cultivar in the environment	0 to 1 by .01
$\sigma_{S,R}$	Cultivars selectivity ratio (σ_S/σ_R)	0.1 to 1 by .02 step
$\alpha_{S,R}$	The distance between μ_S and μ_R ($\lvert\mu_S - \mu_R\rvert$)	{0.1, 0.25, 0.3, 0.5 }
μ_R	The optimal phenotypic value on the R cultivar	$\mu_S + \alpha_{SR}$
$1/\sigma_R^2$	The selectivity of R cultivar	$(\sigma_{S,R}/\sigma_S)^2$
$\rho_{S,R}$	Trade-off strength between S and R cultivars	$\alpha_{S,R}/\sqrt{2(\sigma_S^2+\sigma_R^2)}$
TSR scenario		
$\beta_S(x)$, $\beta_R(x)$	Infection efficiency of the pathogen strain x on S and R cultivars	$3 \cdot 10^{-3}$
$p_S(x)$	Sporulation rate of the pathogen strain x on S cultivar	$20 \cdot G(\mu_S, \sigma_S)(x)$
$p_R(x)$	Sporulation rate of the pathogen strain x on R cultivar	$20 \cdot G(\mu_R, \sigma_R)(x)$
TIE scenario		
$\beta_S(x)$	Infection efficiency of the pathogen strain x on S cultivar	$3 \cdot 10^{-3} \cdot G(\mu_S, \sigma_S)(x)$
$\beta_R(x)$	Infection efficiency of the pathogen strain x on R cultivar	$3 \cdot 10^{-3} \cdot G(\mu_R, \sigma_R)(x)$
$p_S(x)$, $p_R(x)$	Sporulation rate of the pathogen strain x on S and R cultivars	20

Table 2: Parameters used for the simulations with two host classes (S and R cultivars). Two scenarios were considered: the R cultivar can either alter the Infection Efficiency (TIE) or the Sporulation Rate (TSR).

4.2 Evolutionary dynamics with R genes altering sporulation rate (TSR)

Let us first consider a quantitative R gene altering the sporulation rate of a fungal pathogen. Three cases corresponding to three shapes of the fitness function Ψ, differing by the number of modes and their steepness, are considered in

turn (Figure 2). If at equilibrium the population always becomes monomorphic around an endpoint characterized by Ψ, its shape impacts the duration of the transient dynamics

Case 1: The fitness function Ψ is unimodal. For a weak trade-off $\rho_{S,R} < 1$, Ψ has a unique local maximum point at $\mu^*(\mu_S < \mu^* < \mu_R)$ which is the unique evolutionary endpoint (Figure 2 A). It corresponds to a generalist pathogen. Simulations show a fast transient dynamics concentrating rapidly the pathogen population around μ^* (Figure 2 B,C). It corresponds to a fast erosion of the quantitative R as measured by T_{inf} (Figure 2 C).

Case 2: The fitness function Ψ is bimodal with a unique global maximum. For a strong trade-off $\rho_{S,R} > 1$, Ψ is maximized (globally) by a single phenotypic value μ_R, but a local maximum also exists around μ_S (Figure 2 D). The $\mathcal{R}_0$ maximization principle shows that μ_R is the evolutionary endpoint. This phenotype is a specialist of the R cultivar. Here, the pathogen population lives for a relatively long time at low densities around the initially dominant phenotypic value μ_S and then shifts by mutation on μ_R (Figure 2 E,F). These dynamics occur simultaneously on the S and R cultivars. The durability of the R cultivar (as measured by T_{inf}) can be relatively long if the R cultivar remained firstly dimly (and decreasingly) infected. Notice that the pathogen phenotypic shift (as measured by T_{shift}) (Figure 2 F) just before T_{inf}. However, other proportion of R cultivar φ can lead to much lower durability if they bring closer the fitness peaks (in the sens $\Psi(\mu_S) \lessapprox \Psi(\mu_R)$) as illustrated in Figure 2 G-I. Notice also that T_{shift} occurs here much later.

Case 3: The fitness function Ψ is bimodal with two global maxima. The two global maxima μ_S and μ_R of Ψ are evolutionary attractors (Figure S1 A). The $\mathcal{R}_0$ maximization principle does not permit to characterize the evolutionary endpoint. However, we can calculate the effect of mutation on pathogen fitness Ψ^ε (see (E.10)) and then, the sign of the difference $\Psi^\varepsilon(\mu_S) - \Psi^\varepsilon(\mu_R)$ allow to go a step further. The S and R cultivars differed by their selectivities ($1/\sigma_S^2 > 1/\sigma_R^2$, meaning that $\Psi''(\mu_S) < \Psi''(\mu_R)$). It comes that $\Psi^\varepsilon(\mu_R) > \Psi^\varepsilon(\mu_S)$ for ε sufficiently small: μ_R is thus the evolutionary endpoint. Graphically, it corresponds to the less selective (*i.e.* flatter) fitness peak. The pathogen phenotypes indeed concentrate around μ_R in the long-time dynamics (Figure S1 B,D) but remained a much longer time than previously (Figure S1 B,D versus Figure 2 D-I) around the initially dominant phenotype μ_S. However this fitness configuration is not robust. The slightest perturbation of host selectivities easily rules out the predicted transient dynamics.

$\varphi = 0.52,\ \rho_{S,R} = 0.83$

$T_{\text{inf}} = 1.2,\ T_{\text{shift}} = \text{NA},\ R_0(\mu_S) = 1.73,\ R_0(\mu_R) = 1.82$

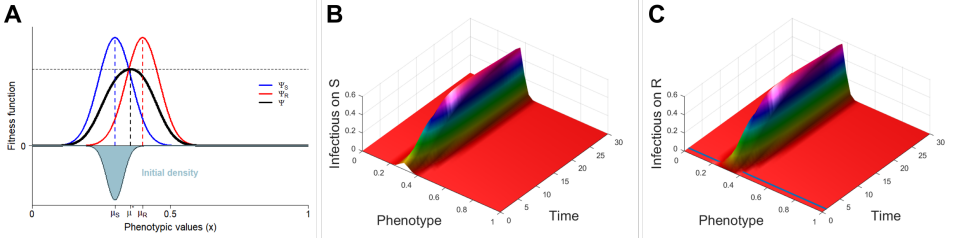

$\varphi = 0.62,\ \rho_{S,R} = 2.7$

$T_{\text{inf}} = 131,\ T_{\text{shift}} = 123,\ R_0(\mu_S) = 1.08,\ R_0(\mu_R) = 1.47$

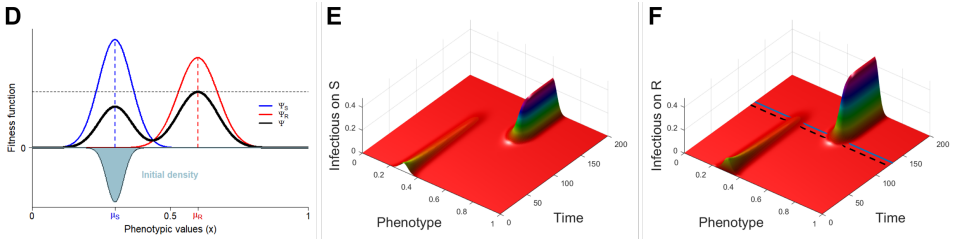

$\varphi = 0.56,\ \rho_{S,R} = 2.7$

$T_{\text{inf}} = 1.5,\ T_{\text{shift}} = 576,\ R_0(\mu_S) = 1.25,\ R_0(\mu_R) = 1.33$

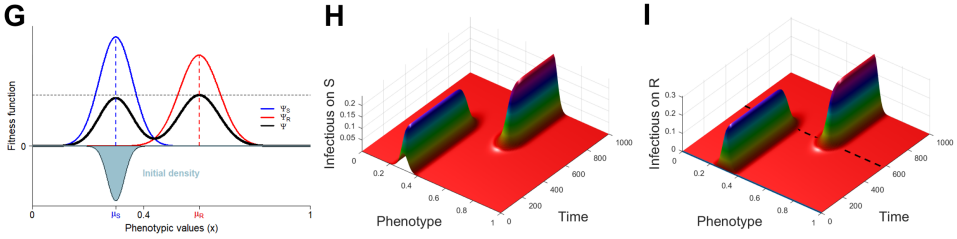

Figure 2: Evolutionary epidemiology dynamics when the resistance impacts the pathogen sporulation function p_k for three configurations of the fitness function Ψ. **A-C** The fitness function is unimodal: $\sigma_S = \sigma_R = 0.06$; $\mu_S = 0.3$; $\mu_R = 0.4$. At $t = 0$, the pathogen population, essentially concentrated around the phenotypic value μ_S, is adapted on the S cultivar. The dynamics of the density of infected tissue and the phenotypic composition of the pathogen population in the S and R cultivars are display in B and C, respectively. Panels D-F and G-I are organized similarly. **D-F** and **G-I** The fitness function is bimodal with a unique global maximum μ_R ($\sigma_S = 0.06$, $\sigma_R = 0.072$; $\mu_S = 0.3$; $\mu_R = 0.6$) but a local maximum also exists around μ_S. The value of φ in panels G-I (0.56) implied that μ_S is more closer to μ_R compared to panels D-F where $\varphi = 0.62$. In panels C,F,I the blue line represents T_{inf} and the dash-black line T_{shit}.

4.3 Evolutionary dynamics with R genes altering infection efficiency (TIE)

Let us now consider a quantitative R gene altering infection efficiency. Evolutionary endpoints and transient dynamics remain overall unchanged for the case 1. Substantial differences occurr in cases 2 and 3. In sharp contrast with the TSR scenario, the pathogen population can be monomorphic or dimorphic at equilibrium. A dimorphic equilibrium is for example observed in Figure 3 E,F and H,I and Figure S1 C,E. Formally, dimorphism occurs if and only if there exists two constants $a_S, a_R > 0$ defined by system (F.13) (Appendix F). From an epidemiological point a view, a dimorphism occurs if $\mathcal{R}_0^R(\mu_R) > 1$ and $\mathcal{R}_0^S(\mu_S) > 1$ where $\mathcal{R}_0^k(x)$ is the basic reproduction number of the pathogen phenotype x in the environment k (defined by (3.4)).

Choosing a R gene targeting infection efficiency protects the R cultivar from any infection during a long initial period measured by T_{inf} (Figure 3 F,I). Indeed, each cultivar is infected by a specific strain. At equilibrium, the pathogen population is composed by different proportions of the two evolutionary attractors μ_S and μ_R (Figure 3 E,F and H,I and Figure S1 C,E). This is not the case for a R gene targeting sporulation rate as the R cultivar can then be infected from the very start of its deployment (Figure 2 F,I and Figure S1 D). Indeed, the S and R cultivars are simultaneously infected by the same pathogen strain which phenotype can change with time (Figure 2 D-I). Depending on φ, durability T_{inf} can be close for the TSR and TIE scenarii (Figures 2 F versus 3 F) or much higher with the TIE scenarii as soon as φ brings fitness peaks closer (Figures 3 I versus 2 I).

4.4 Strategies for plant resistance management

A deployment strategy is characterized by (1) the choice of the R gene, which depends on the targeted pathogenicity trait and on the trade-off $\rho_{S,R}$, and (2) the proportion φ of the R cultivar cultivated in the environment. We have just illustrated that the transient evolutionary dynamics depends on these factors. Here we extend this analysis by plotting these factors in the plane $(\varphi, \rho_{S,R})$.
Resistance durability differ substantially between the TIE (R genes altering infection efficiency) and TSR (R genes altering sporulation rate) scenarii. A large plateau of high durability along the secondary diagonal exists with TIE scenario (Figure 4 A). Its upper boundary (*i.e.* high φ and $\rho_{S,R}$ values) is sharply delimited by the area where $R_0(\mu_R) < 1$ (Figure 4 C). Its lower boundary (*i.e.* low φ and $\rho_{S,R}$ values) delimits an area of very low durability corresponding mostly to the fast invasion of a generalist pathogen ($R_0(\mu_*) < 1$) (Figure 4 C). The picture is highly different for R genes altering sporulation rate (TSR scenario) (Figure 4 B). A plateau of high durability exists only in the area where $R_0(\mu_S) < 1$ and $R_0(\mu_R) < 1$ (Figure 4 D). In this zone, epidemics go extinct following the deployment of the R cultivar in a large proportion of the environment. Elsewhere resistance durability is mirroring the absolute difference $R_0(\mu_R) - R_0(\mu_S)$, especially when $R_0(\mu_R) < 1$. The epidemiological protection,

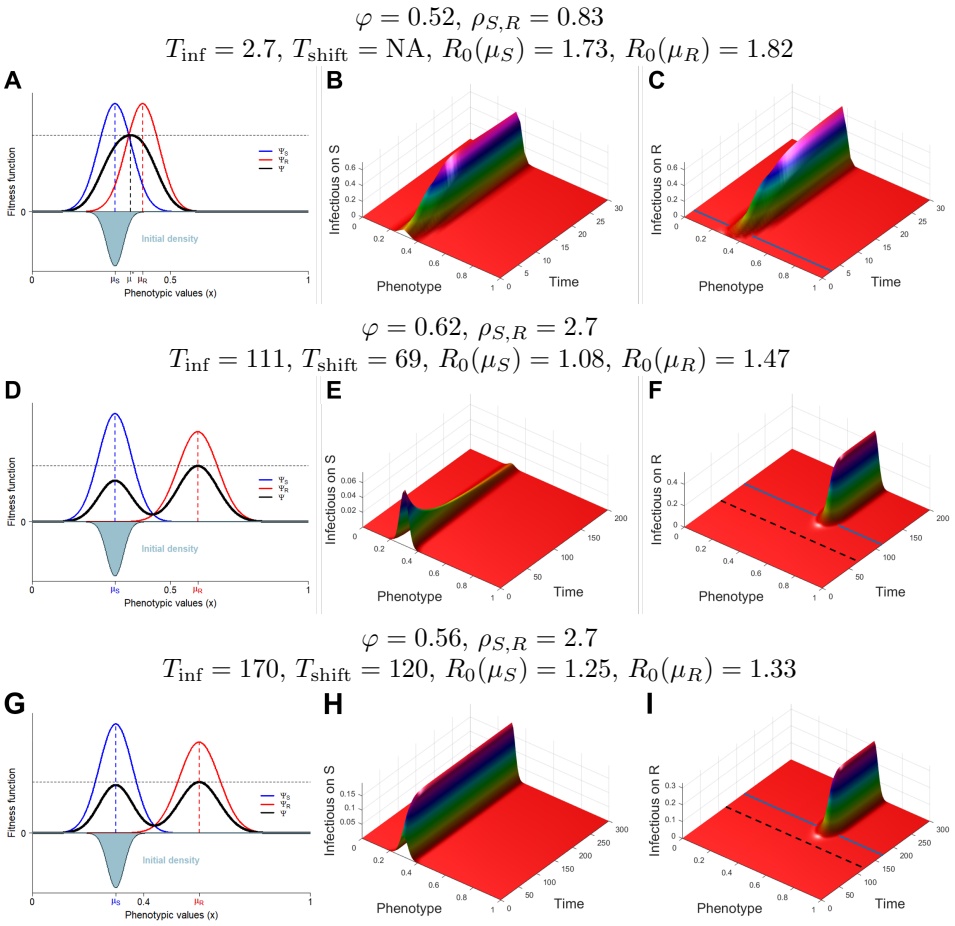

Figure 3: Evolutionary epidemiology dynamics when the resistance impacts the pathogen infection efficiency β_k for three configurations of the fitness function Ψ. **A-C** The fitness function is unimodal: $\sigma_S = \sigma_R = 0.06$; $\mu_S = 0.3$; $\mu_R = 0.4$. At $t = 0$, the pathogen population, essentially concentrated around the phenotypic value μ_S, is adapted on the S cultivar. The dynamics of the density of infected tissue and the phenotypic composition of the pathogen population in the S and R cultivars are display in B and C, respectively. Panels D-F and G-I are organized similarly. **D-F** and **G-I** The fitness function is bimodal with a unique global maximum μ_R ($\sigma_S = 0.06$, $\sigma_R = 0.072$; $\mu_S = 0.3$; $\mu_R = 0.6$) but a local maximum also exists around μ_S. The value of φ in panels G-I (0.56) implied that μ_S is more closer to μ_R compared to panels D-F where $\varphi = 0.62$. In panels C,F,I the blue line represents T_{inf} and the dash-black line T_{shit}.

estimated by the relative HAD obtained when deploying a R cultivar, is also of major interest as it is a proxy of crop yield. The relative HAD are quite close for both scenarii (Figure 4 E,F), mirroring the absolute value of $R_0(\mu_R) - R_0(\mu_S)$ (Figure 4 D). However, interestingly, crop yields are always higher, in average of 13%, with R gene targeting infection efficiency. Over the 7826 simulations performed for each scenario, the ratio between relative HAD for the TIE and TSR cases range from 1 to 1.24 (mean=1.13, sd=0.08). The general picture just described for a phenotypic distance between optimal phenotypes ($|\mu_S - \mu_R|$) of 0.25, is conserved for a doubled phenotypic distance (Figure S2), corresponding to a situation where more mutations are required for pathogen adaptation.

5 Discussion

This work follows an ongoing trend aiming to jointly model the epidemiological and evolutionary dynamics of host-parasite interactions. Our theoretical framework, motivated by fungal infections in plants, allows us to tackle the question of the durability of plant quantitative resistance genes altering specific pathogen life-history traits. Many problems and questions are reminiscent of the literature on the epidemiological and evolutionary consequences of vaccination strategies. For instance, quantitative resistance traits against pathogen infection rate, latent period and sporulation rate are analogous to partially effective (imperfect) vaccines with anti-infection, anti-growth or anti-transmission modes of action, respectively (Gandon et *al.*, 2001). Similarly, the proportion of fields where a R cultivar is deployed is analogous to the vaccination coverage in the population (Gandon & Day, 2007).

Evolutionary outcomes with multimodal fitness functions. In line with early motivations for developing a theory in evolutionary epidemiology (Day & Proulx, 2004), we investigated both the short- and long-term epidemiological and evolutionary dynamics of the host-pathogen interaction. Although the short-term dynamics is investigated numerically, the long-term analysis is analytically tractable and allows us to predict the evolutionary outcome of pathogen evolution. In contrast with most studies in evolutionary epidemiology, the analysis proposed allows us to consider multimodal fitness functions, and to characterize evolutionary endpoints thought of a detailed description of the shape of fitness function (number of modes, steepness and any higher moments with even order). Similarly, our results are neither restricted to Gaussian mutation kernel m (see also Mirrahimi (2017)), provided that m is symmetric and positive (Appendix B), nor to rare mutations as in the classical adaptive dynamics approach.
An important consequence of our model assumptions is that the model admits an optimisation principle (Mylius & Diekmann, 1995; Metz et *al.*, 2008; Lion & Metz, 2018). In other words, the evolutionary attractors of our model coincide with the maxima of a particular function, which can be viewed as a measure of absolute fitness. Here, the function $\Psi(x)$, or equivalently, the basic reproduction

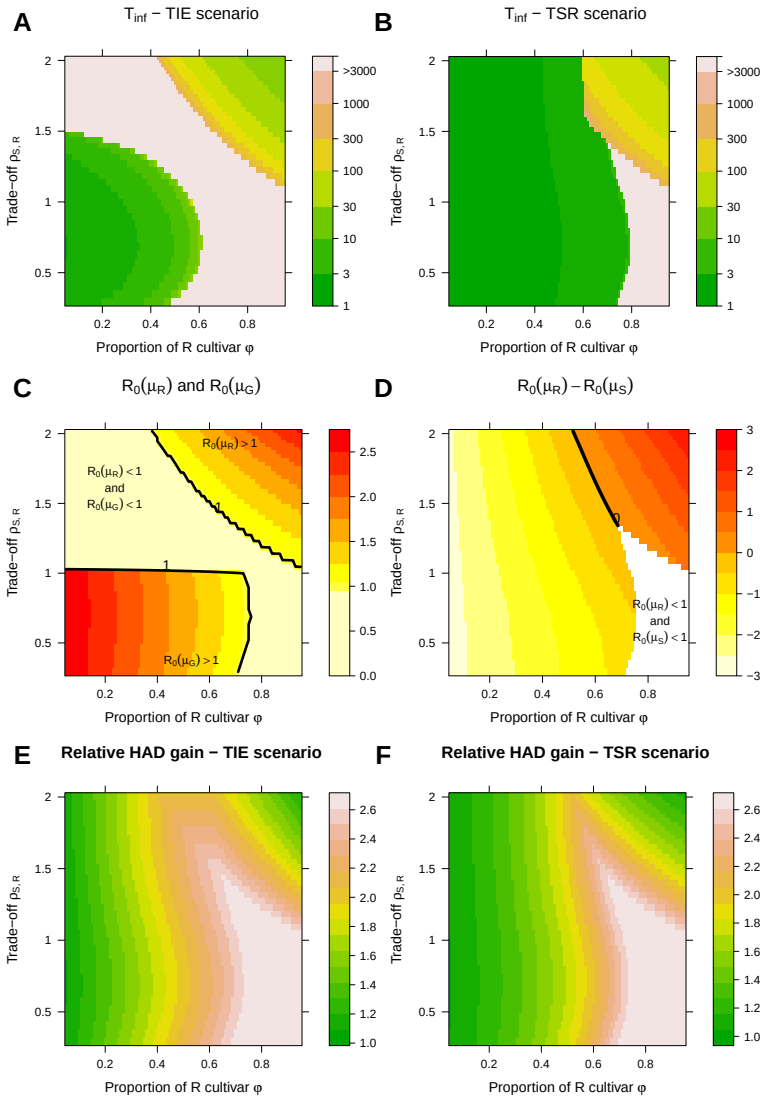

Figure 4: Effects of the proportion φ of R cultivar, the pathogenicity trait targeted by R gene and the adaptation trade-off $\rho_{S,R}$ on resistance durability, basic reproduction numbers and epidemiological protection. The phenotypic distance $|\mu_S - \mu_R|$ is fixed to 0.25, a situation where a few mutations are required for pathogen adaptation. **A** Resistance durability as measured by the time of the beginning of the R gene erosion (T_{inf}, log scale) for a resistance altering infection efficiency (TIE scenario). **B** Same as **A** for a resistance altering sporulation rate (TSR scenario). **C** Basic reproduction numbers of the pathogen phenotype values μ_R (specialist, $\rho_{S,R} > 1$) and μ_G (generalist, $\rho_{S,R} < 1$). **D** Difference between the basic reproduction numbers of the pathogen phenotype values μ_R and μ_S. **E** Epidemiological protection for the TIE scenario as measured by the relative HAD. **F** Same as **E** for the TSR scenario.

ratio $R_0(x)$ in a fully susceptible population, plays this role. Potential evolutionary attractors are located at the peaks of the landscape represented by this function. The interplay between mutation and selection then determines the composition of the population at equilibrium, although a general conclusion of our work is that the population will generically concentrate around the highest peak. In our work, the TSR model admits an optimisation principle, whereas for the TIE model the function $\Psi(x)$ is only an approximate optimisation principle. However, the existence of an optimisation principle in both models is guaranteed by the specific form of environmental feedback: in the fitness proxy $R(x, y)$, the densities of susceptible hosts in each class, $S_k(x)$, are all decreasing function of a single environmental variable, the density of spores in the pool of propagules. Hence, the environmental feedback loop is effectively one-dimensional and the model admits an optimisation principle (Mylius & Diekmann, 1995; Metz et *al.*, 2008; Lion & Metz, 2018). An important consequence of the existence of an optimisation principle is that evolutionary branching (*i.e.* a situation leading to pathogen diversification and to long term coexistence of different pathogen strategies) is impossible. As a result only neutral coexistence (as observed when the function $\Psi(x)$ has two global maxima) is possible.

R_0 expression for fungal pathogens in heterogeneous environment. Our model yields a fitness proxy for fungal pathogens, the function $\Psi(x)$, which is proportional to the basic reproduction ratio $R_0(x)$. Usually, the computation of $\mathcal{R}_0$ is based on the spectral radius of the next generation operator (NGO), (Diekmann et *al.*, 1990; Diekmann & Heesterbeek, 2000). The method was applied by Van den Bosch et *al.* (2008) to calculate the $\mathcal{R}_0$ for lesion forming foliar pathogens in a setting with only two cultivars and no effect of the age of infection a on sporulation rate and disease-induced mortality. Here, we follow the methodology based on the generation evolution operator (Inaba, 2012) to derive an expression for the basic reproduction ratio $\mathcal{R}_0$ in heterogeneous host populations composed of n_c cultivars (see Appendix D for more details).
Equations (3.4), either with (3.6) or with (3.7), provides $\mathcal{R}_0(x)$ expressions for the two classical models of sporulation curve proposed by Segarra et *al.* (2001) (Figure 1 A). They combine (i) the pathogenicity traits expressed at the scale of the plant during the basic infection steps (infection efficiency $\beta(x)$, latent period $\tau(x)$, sporulation rate $p(x)$ and infectious period $l(x)$ with (ii) the cultivar proportion in the environment (φ_k). As pathogenicity traits can be measured in the laboratory, $\mathcal{R}_0(x)$ bridges the gap between plant-scale and epidemiological studies and between experimental and theoretical approaches. $\mathcal{R}_0$-based approach have been for example used to compare the fitness of a collection of isolates of potato light blight (Montarry et *al.*, 2010), to highlight the competition exclusion principle for multi-strains within-host malaria infections (Djidjou-Demasse & Ducrot, 2013) and to predict the community field structure of Lyme disease pathogen from laboratory measures of the three transmission traits (Durand et *al.*, 2017). Lannou (2012) pointed out the need for $\mathcal{R}_0(x)$ expressions allowing to compare the fitness of competing pathogen strains with different latent peri-

ods. We showed that our $\mathcal{R}_0$ expressions are exact fitness proxy for competing strains differing for 3 pathogenicity traits (latent period, sporulation rate or infectious period) but only an approximation for strains differing for their infection efficiencies. More generally, a clear distinction between pathogen invasion fitness $\mathcal{R}(x, y)$ and epidemiological $\mathcal{R}_0(x)$ is necessary to properly discuss the adaptive evolution of pathogens (Lion & Metz, 2018).

Sustainable management of plant quantitative resistance. Only few studies compared the effects on disease management of R cultivars targeting different aggressiveness component of plant fungal pathogens while taking into account evolutionary principles (Iacono et *al.*, 2012; Bourget *al.*, 2015; Rimbaud et *al.*, 2018). Depending on stakeholders objectives, two main criteria are used in the literature (Van den Bosch & Gilligan , 2003; Papaïx et *al.*, 2018): (i) the epidemiological protection (relative HAD) and (ii) resistance durability (T_{inf}). Importantly, we illustrated how these criteria are related to the corner-stone concept of basic reproduction ratio $R_0(x)$. Both epidemiological protection and resistance durability are obviously favored by deployment strategies lessening $\mathcal{R}_0(\mu_S)$ and $\mathcal{R}_0(\mu_S)$ below one. Originally, when $\mathcal{R}_0(\mu_S) > 1$ or $\mathcal{R}_0(\mu_S) > 1$, our results highlight how to take advantage of neutral coexistence (*i.e.* $|R_0(\mu_R) - R_0(\mu_S)| \approx 0$) to increase the epidemiological protection provided by quantitative resistance (*e.g.* Figure 4 D-F).
Iacono et *al.* (2012) and Rimbaud et *al.* (2018) already reported that quantitative resistance reducing the infection efficiency provides a greater epidemiological protection than quantitative resistance that reduces the sporulation rate. Our results are consistent with these studies and go one step further by analyzing the underlying transient evolutionary dynamics. In the plane $(\varphi, \rho_{S,R})$, positioning two main parameters of deployment strategies, high resistance durability is far less frequent for R genes targeting the sporulation rate. This difference is blurred by $R_0(x)$ expressions where both traits appear as a product $\beta_k \times p_k$ (see equation (3.5)). As advised by Pilet-Nayel et *al.* (2017), these comparisons can guide plant breeders to adequately choose resistance QTLs in breeding programs. Compared to Papaïx et *al.* (2018); Rimbaud et *al.* (2018), the results exemplified with a different modeling approach (stochastic demo-genetic models *v.s.* deterministic integro-differential model) that resistance durability criteria and epidemiological protection criteria are not necessarily correlated (Figure 4 A,B versus E,F), and thus, can be associated to incompatible management objectives (Papaïx et *al.*, 2018). Moreover, it is worth noting that, although we did not explore this possibility, our analytical and simulation framework could be used to deal with correlations between traits. In the model, trade-offs between the pathogen life-history traits emerge from the covariance matrix of the (multidimensional) mutation kernel m (Gandon , 2004). This is an important feature that deserve further studies as such correlations are observed for plant fungi (Pariaud et *al.* (2009); Lannou (2012)). Finally, the model is well-suited to derive the equations of evolution of the pathogen life history traits on the same time-scale than epidemiological processes (Day & Gandon, 2006; Day &

Proulx, 2004). It could for example help designing evolution experiments by providing testable hypotheses given that genetic variance-covariance matrix of pathogenicity traits can be estimated.

Notes on some model assumptions. The model assumes an infinite size for the pathogen population. With finite population size, stochastic dynamics can greatly impact evolutionary dynamics (*e.g.*. lower probabilities of emergence and fixation of beneficial mutations, reduction of standing genetic variation (Kimura, 1962). In particular, genetic drift is more likely to impact the maintenance of a neutral polymorphism, as observed here with neutral coexistence, rather than of a protected polymorphism where selection favors coexistence of different genotypes against invasions by mutant strategies (Geritz et *al.*, 1998). However, the effect of genetic drift depends on the stability properties of the model considered. As our model has a unique globally stable equilibrium, genetic drift is likely to play a much lesser role than with models characterized by unstable equilibrium. In practice, the magnitude of genetic drift depends on the effective population size (N_e) of the pathogen population considered (Charlesworth, 2009). Large N_e have been reported at field scale for wind-dispersed, spore-producing plant fungal pathogens (*e.g.* 998 for *Magnaporthe oryzae* (Ali et *al.*, 2016), 3800 to 4400 for *Zymoseptoria tritici* (Zhan et *al.*, 2001) and 1261 to 25258 for *Botrytis cinerea* (Walker et *al.*, 2017)). Ignoring drift seems thus reasonable for those pathogens, at least when considering the fate of new strains with selection coefficient $> 10^{-3}$ as evolution is mostly deterministic when the product of N_e and of the intensity of selection selection is > 1 (Charlesworth (2009)).

As addressed previously, the one-dimensional environmental feedback loop of the model is ensured by assuming an unique pool of propagules. Space is thus implicit, meaning that the probability for a spore of migrating from one point of the environment to another does not depend on their distances. In practice, this assumption is more likely when the extent of the field or landscape considered is not too large with respect to the dispersal function of airborne propagules. Airborne fungal spores often disperse over substantial distances with mean dispersal distance in the order of one kilometer (*e.g.* 0.2-14 km for *Mycosphaerella fijiensis* (Rieux et *al.*, 2014)), 0.86 km for *Podosphaera plantaginis* (Soubeyrand et *al.*, 2009), 1.4-2.6 km for *Hymenoscyphus fraxineus* Grosdidier et *al.* (2018)) and, in most case, fat-tail dispersal kernels associated to substantial long-distance dispersal events. For other pathosystems however, limited dispersal may be an important epidemiological process, and it would be interesting to extend our approach to a spatially explicit environment drawing upon, for example, the recent model of Mirrahimi (2017) describing a phenotypically structured population subject to mutation, selection and migration between two habitats. Indeed, when dispersal decreases with distance, large homogeneous habitats promote diversification while smaller habitats, favoring migration between distinct patches, hamper diversification Débarre & Gandon (2010); Haller et *al.* (2013); Papaïx et *al.* (2013). Pathogen diversification, which results from evolutionary

branching, is of practical importance for management purposes, as evidenced in the wheat rust fungal disease, where disease prevalence varies with the frequencies of specialist genotypes in the rust population (Papaïx et *al.*, 2011). More generally, managing population polymorphisms, either for conservation purpose in order to preserve the adpative potential of endangered species or for disease control purpose in order to hamper pest and pathogen adaptation is becoming a growing concern (Vale, 2013).

Acknowledgements

Authors thank Loup Rimbaud for comments and suggestions on the manuscript.

Code availability

The MATLAB and R scripts used to simulate the model and generate the figures have been deposited in Dataverse at https://doi.org/10.15454/WAEIMA

Funding

R.D.D. received support from the Conseil Interprofessionnel du Vin de Bordeaux (CIVB) under the CIVB project 'Recherche, experimentation, etudes et outils', and from the EU in the framework of the Marie-Curie FP7 COFUND People Programme, through the award of an AgreenSkills/AgreenSkills+ fellowship under grant agreement number FP7-609398.

References

Anderson, P.K., Cunningham, A.A., Patel, N.G., Morales, F.J., Epstein, P.R. and Daszak, P. 2004. Emerging infectious diseases of plants: pathogen pollution, climate change and agrotechnology drivers. Trends in Ecology & Evolution, 19, 535-544.

Ali, S., Soubeyrand, S., Gladieux, P., Giraud, T., Leconte, M., Gautier, A. Mboup, M., Chen, W., Vallavieille-Pope, C. and Enjalbert, J. 2016. cloncase: Estimation of sex frequency and effective population size by clonemate resampling in partially clonal organisms. Molecular Ecology Resources, 16, 845-861.

Anderson, R. M. 1991. Populations and Infectious Diseases: Ecology or Epidemiology? Journal of Animal Ecology, 60, 1-50.

Barrett, L. G., Thrall, P. H., Burdon, J. J., and Linde, C. C. 2008. Life history determines genetic structure and evolutionary potential of host–parasite interactions. Trends in Ecology & Evolution, 23(12), 678-685.

Behboodian, J. 1970. On the modes of a mixture of two normal distributions. Technometrics, 12(1), 131-139.

Bourget, R., Chaumont, L., Durel, C-E. and Sapoukhina, N. 2008. Sustainable deployment of QTLs conferring quantitative resistance to crops: first lessons from a stochastic model. New Phytologist, 206(3), 1163–1171

Charlesworth, B. 2009. Effective population size and patterns of molecular evolution and variation. Nature Reviews Genetics, 10, 195-205.

David, O., Lannou, C., Monod, H., Papaïx, J., and Traore, D. 2017. Adaptive diversification in heterogeneous environments. Theoretical population biology, 114, 1-9.

Day, T. 2002. Virulence evolution via host exploitation and toxin production in spore-producing pathogens. Ecology Letters, 5(4), 471-476.

Day, T., and Proulx, S. R. 2000. A general theory for the evolutionary dynamics of virulence. The American Naturalist, 163(4), e40-63.

Day, T., Gandon, S. 2006. Insights from Price's equation into evolutionary. Disease evolution: models, concepts, and data analyses, 71, 23.

Débarre, F., and Gandon, S. 2010. Evolution of specialization in a spatially continuous environment. Journal of evolutionary biology, 23(5), 1090-1099.

Diekmann, O., Heesterbeek, J. A. P. and Metz, J. A. 1990. On the definition and the computation of the basic reproduction ratio R0 in models for infectious diseases in heterogeneous populations. Journal of mathematical biology, 28(4), 365-382.

Dieckmann, O. and Heesterbeek, J. P. 2000. Mathematical epidemiology of infectious diseases: Model building, Analysis and Interpretation, Wiley, Chichester, UK.

Diekmann, O., Jabin, P.E., Mischler, S. and Perthame, B. 2005. The dynamics of adaptation: an illuminating example and a Hamilton-Jacobi approach. Theoretical Population Biology, 67, 257-271.

Dieckmann, U. 2002. Adaptive dynamics of pathogen-host interactions. In U. Dieckmann, J. A. J. Metz, M. W. Sabelis et K. Sigmund (eds), Adaptive dynamics of infectious diseases: In pursuit of virulence management. Cambridge University Press, pp. 39-59.

Djidjou Demasse, R. and Ducrot, A. 2013. An age-structured within-host model for multistrain malaria infections. SIAM Journal of Applied Mathematics, 73, 572-593.

Djidjou-Demasse, R., Ducrot, A. and Fabre, F. 2017. Steady state concentration for a phenotypic structured problem modeling the evolutionary epidemiology of spore producing pathogens. Mathematical Models and Methods in Applied Sciences, 27(02), 385-426.

Durand, J., Jacquet, M., Rais, O., Gern, L., and Voordouw, M. J. 2017. Fitness estimates from experimental infections predict the long-term strain structure of a vector-borne pathogen in the field. Scientific reports, 7(1), 1851.

Fisher, R. A. 1930. The genetical theory of natural selection. Oxford University Press, Oxford, U.K.

Gandon, S., Mackinnon, M.J., Nee, S. and Read, A.F. 2001. Imperfect vaccines and the evolution of pathogen virulence. Nature. 414(6865), 751–756.

Gandon, S. 2004. Evolution of Multihost Parasites. Evolution, 58(3), 455-469.

Gandon, S. and Day, T. 200). The evolutionary epidemiology of vaccination. Journal of the Royal Society Interface, 4(16), 803-817.

Geritz, S.A., Metz, J.A., Kisdi, É. and Meszéna, G. 1997. Dynamics of adaptation and evolutionary branching. Physical Review Letters, 78(10), 2024-2027.

Geritz, S.A.H., Kisdi, É., Meszéna, G. and Metz, J.A.J. 1998. Evolutionarily singular strategies and the adaptive growth and branching of the evolutionary tree. Evolutionary Ecology, 12, 35-57.

Giraud, T., Gladieux, P. and Gravrilets, S. 2010. Linking the emergence of fungal plant diseases with ecological speciation. Trends in Ecology & Evolution, 25, 387-395.

Grosdidier, M., Ioos, R., Husson, C., Cael, O., Scordia, T. and Marçais, B. 2018. Tracking the invasion: dispersal of Hymenoscyphus fraxineus airborne inoculum at different scales. FEMS Microbiology Ecology, 94, fiy049.

Haller, B.C., Mazzuccco, R. and Dieckmann, U. 2013. evolutionary branching in complex landscape. American Naturalist, 184(4), e127-141.

Iacono, G.L., van den Bosch, F. and Paveley, N. 2012. The evolution of plant pathogens in response to host resistance: factors affecting the gain from deployment of qualitative and quantitative resistance. Journal of Theoretical Biology, 304, 152-163.

Inaba, H. 2012. On a new perspective of the basic reproduction number in heterogeneous environments. Journal of mathematical biology, 65(2), 309-348.

Kimura, M. 1962. On the probability of fixation of mutant genes in a population. Genetics, 47, 713-719.

Lannou, C. 2012. Variation and selection of quantitative traits in plant pathogens. Annual Review of Phytopathology, 50, 319-338.

Lion, S. and Metz, J. A. J. 2018. Beyond R_0 maximisation: on pathogen evolution and environmental dimensions. Trends In Ecology & Evolution, 33, 75-90.

Macarthur, R., and Levins, R. 1967. The limiting similarity, convergence, and divergence of coexisting species. The American Naturalist, 101(921), 377-385.

Martin, G. and Lenormand, T. 2006. A general multivariate extension of Fisher's geometrical model and the distribution of mutation fitness effects across species. Evolution, 60, 893-907.

McDonald, B. A. and Linde, C. 2002. Pathogen population genetics, evolutionary potential, and durable resistance. Annual review of phytopathology, 40(1), 349-379.

Metcalf, C. J. E., Birger, R. B., Funk, S., Kouyos, R. D., Lloyd-Smith, J. O., and Jansen, V. A. A. 2015. Five challenges in evolution and infectious diseases. Epidemics, 10, 40-44.

Metz, J.A.J., Geritz, S.A.H., Meszéna, G., Jacobs, F.J.A. and van Heerwaarden, J.S. 1996. Adaptive dynamics, a geometrical study of the consequences of nearly faithful reproduction. In: van Strien, S.J., Verduyn Lunel, S.M. (Eds.), Stochastic and spatial Structures of Dynamical Systems. North-Holland, Amsterdam, pp. 183-231.

Metz, J. A. J., Mylius, S. D., & Diekmann, O. (2008). When does evolution optimise? Evolutionary Ecology Research, 10: 629–654

Montarry, J., Hamelin, F.M., Glais, I., Corbière, R. and Andrivon, D. 2010. Fitness costs associated with unnecessary virulence factors and life history traits: evolutionary insights from the potato late blight pathogen Phytophthora infestans. BMC Evolutionary Biology, 10, 1-9.

Mirrahimi, S. 2017. A Hamilton–Jacobi approach to characterize the evolutionary equilibria in heterogeneous environments. Mathematical Models and Methods in Applied Sciences, 27(13), 2425-2460.

Mundt, C. 2014. Durable resistance: A key to sustainable management of pathogens and pests. Infection, Genetics and Evolution, 14, 446-455.

Mylius, S. D. and Diekmann, O. 1995. On evolutionarily stable life histories, optimization and the need to be specific about density dependence. Oikos, 218-224..

Niks, R. E., Qi, X. and Marcel, T.C. 2015. Quantitative Resistance to Biotrophic Filamentous Plant Pathogens: Concepts, Misconceptions, and Mechanisms. Annual Review of Phytopathology, 53, 444-470.

Orr, H. A. 2005. The genetic theory of adaptation: a brief history. Nature Reviews Genetics, 6, 119-127.

Pariaud, B., Ravigné, V., Halkett, F., Goyeau, H., Carlier, J. and Lannou, C. 2009. Aggressiveness and its role in the adaptation of plant pathogens. Plant Pathology, 58(3), 409-424.

Papaïx, J., Goyeau, H, Du Cheyron, P., Monod, H and Lannou, C. 2011. Dynamics of Adaptation in Spatially Heterogeneous Metapopulations. New Phytologist, 191(4), 1095-1107.

Papaïx, J., David, O., Lannou, C. and Monod, H. 2013. Dynamics of Adaptation in Spatially Heterogeneous Metapopulations. PLoS ONE, 8(2), e54697.

Papaïx, J., Rimbaud, L., Burdon, J. J., Zhan, J. and Thrall, P. H. 2018. Differential impact of landscape-scale strategies for crop cultivar deployment on disease dynamics, resistance durability and long-term evolutionary control. Evolutionary Applications, 11(5), 705-717.

Poland, J. A., Balint-Kurti, P. J., Wisser, R. J., Pratt, R. C. and Nelson, R. J. 2009. Shades of gray: the world of quantitative disease resistance. Trends in Plant Science, 14, 21-29.

Parlevliet, J. E. 1986. Pleiotropic association of infection frequency and latent period of two barley cultivars partially resistant to barley leaf rust. Euphytica, 35, 267-272.

Pilet-Nayel, M.-L., Moury, B., Caffier, V., Montarry, J., Kerlan, M.-C., Fournet, S., Durel, C.-E. and Delourme, R. 2017. Quantitative Resistance to Plant Pathogens in Pyramiding Strategies for Durable Crop Protection. Frontiers in Plant Science, 8, 21-29.

Raberg, L., Graham, A. L. and Read, Andrew F. 2009. Decomposing health: tolerance and resistance to parasites in animals. Philosophical Transactions of the Royal Society of London. Series B, Biological Sciences, 364, 37–49.

Restif, O. and Koella, J. C. 2004. Concurrent evolution of resistance and tolerance to pathogens. The American Naturalist 164, e90-102.

Richardson, K. L., Vales, M. I., Kling, J. G., Mundt, C. C. and Hayes, P. M. 2006. Pyramiding and dissecting disease resistance QTL to barley stripe rust.Theoretical and Applied Genetics, 113, 485–495.

Rieux, A., Soubeyrand, S., Bonnot, F., Klein, E., Ngando, J. E., Mehl, A., Ravigne, V., Carlier, J. and Bellaire, L. 2014. Long-Distance Wind-Dispersal of Spores in a Fungal Plant Pathogen: Estimation of Anisotropic Dispersal Kernels from an Extensive Field Experiment. PLoS ONE, 9, e103225

Rimbaud, L., Papaïx, J., Rey, J. F., Barrett, L. G. and Thrall, P.H. 2018. Assessing the durability and efficiency of landscape-based strategies to deploy plant resistance to pathogens. Plos Computational Biology, 14(4), e1006067.

Rueffler, C. and Metz, J. A. 2013. Necessary and sufficient conditions for R_0 to be a sum of contributions of fertility loops. Journal of mathematical biology, 66(4-5), 1099-1122.

Segarra, J., Jeger, M. J. and Van den Bosch, F. 2001. Epidemic dynamics and patterns of plant diseases. Phytopathology, 91(10), 1001-1010.

Soubeyrand, S., Laine, A. L., Hanski, I. and Penttinen, A. 2009. Spatiotemporal Structure of Host-Pathogen Interactions in a Metapopulation. The American Naturalist, 174, 308-320.

St. Clair, D. A. 2010. Quantitative disease resistance and quantitative resistance loci in breeding. Annual Review of Phytopathology, 48, 247-268.

Van den Driessche, P. and Watmough, J. 2008. Further notes on the basic reproduction number. Mathematical epidemiology, 159-178, Lecture Notes in Math., 1945, Springer, Berlin.

Van den Bosch, F. and Gilligan, C. A. 2003. Measures of durability of resistance. Phytopathology, 93(5), 616-625.

Van den Bosch, F., McRoberts, N., Van den Berg, F. and Madden, L. V. 2008. The basic reproduction number of plant pathogens: matrix approaches to complex dynamics. Phytopathology, 98(2), 239-249.

Vale, P. F. 2013. Killing them softly: managing pathogen polymorphism and virulence in spatially variable environments. Trends in Parasitology, 29(9), 417-422.

Walker, A.-S., Ravigne, V., Rieux, A., Ali, S., Carpentier, F. and Fournier, E. 2017. Fungal adaptation to contemporary fungicide applications: the case of Botrytis cinerea populations from Champagne vineyards (France). Molecular Ecology, 26, 1919-1935.

Zhan, J., Mundt, C.C. and McDonald B.A. 2001. Using restriction fragment length polymorphisms to assess temporal variation and estimate the number of ascospores that initiate epidemics in field populations of Mycosphaerella graminicola. Phytopathology 91:1011-1017.

Zhan, J., Thrall, P. H., Papaïx, J., Xie, L. and Burdon, J. J. 2015. Playing on a pathogen's weakness: using evolution to guide sustainable plant disease control strategies. Annual Review of Phytopathology, 53, 19-43.

A Supplementary Figures

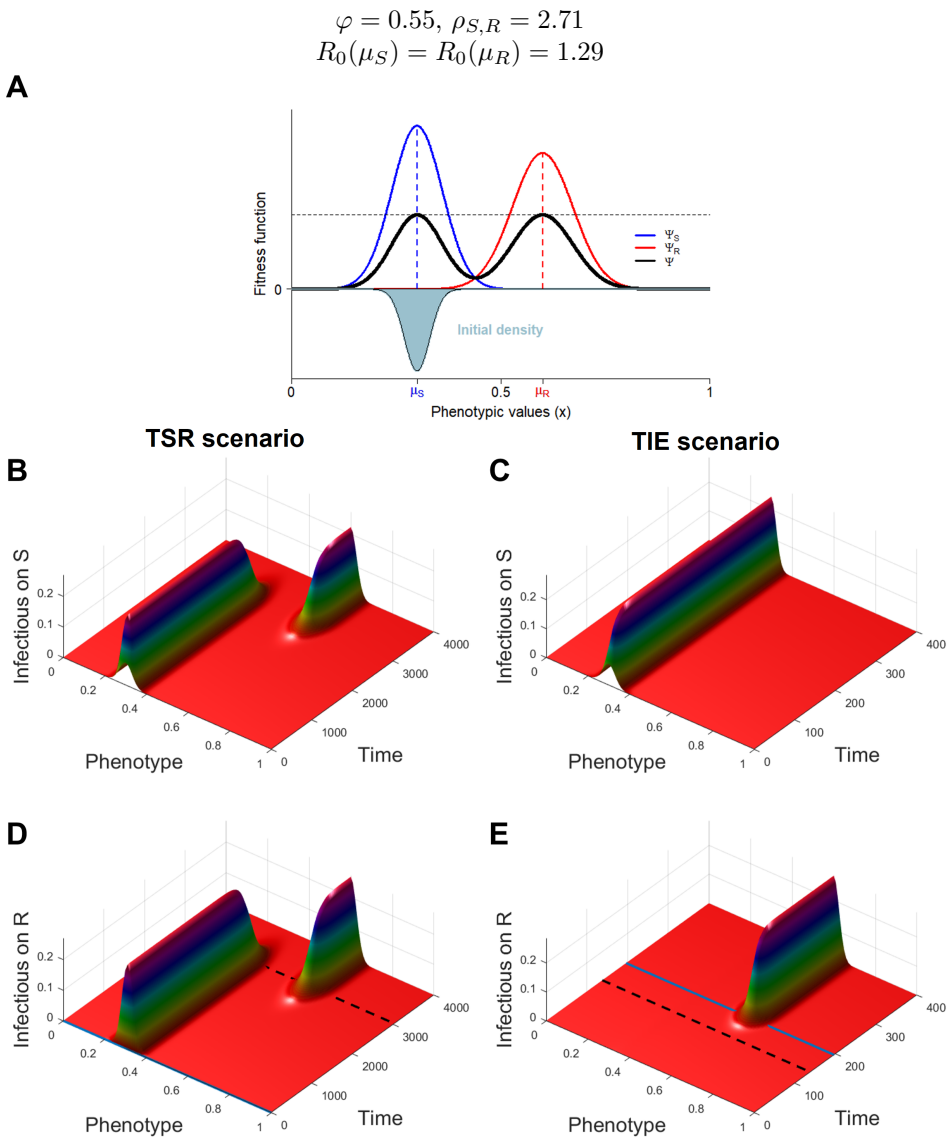

Figure S1: Evolutionary epidemiology dynamics when the resistance impacts the pathogen sporulation rate p_k (TSR scenario) and the infection efficiency β_k (TIE scenario) when the fitness function Ψ is bimodal with two global maxima. **A** The fitness function is bimodal with two maxima: $\sigma_S = 0.06$, $\sigma_R = 0.072$; $\mu_S = 0.3$; $\mu_R = 0.6$. At $t = 0$, the pathogen population, essentially concentrated around the phenotypic value μ_S, is adapted on the S cultivar. The dynamics of the density of infected tissue and the phenotypic composition of the pathogen population in the S and R cultivars are display in B,D (TSR scenario) and C,E (TIE scenario).

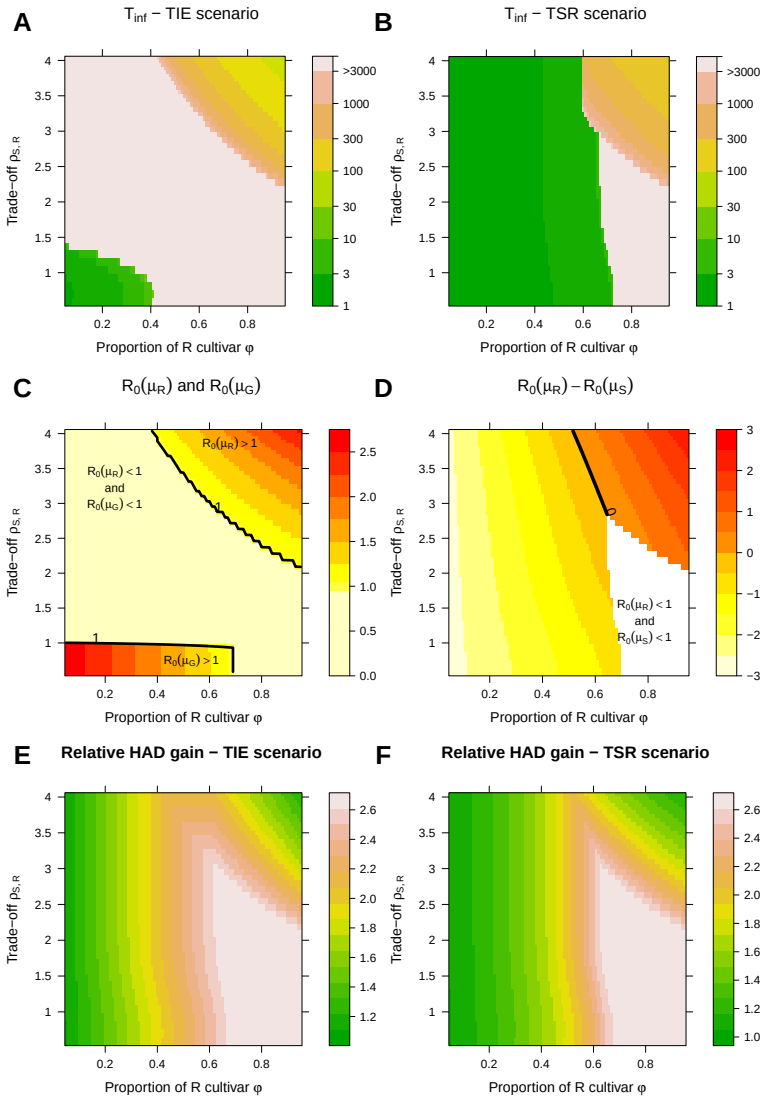

Figure S2: Effects of the proportion φ of R cultivar, the pathogenicity trait targeted by R gene and the adaptation trade-off $\rho_{S,R}$ on resistance durability, basic reproduction numbers and epidemiological protection. The phenotypic distance $|\mu_S - \mu_R|$ is fixed to 0.5, a situation where numerous mutations are required for pathogen adaptation. **A** Resistance durability as measured by the time of the beginning of the R gene erosion (T_{inf}, log scale) for a resistance altering infection efficiency (TIE scenario). **B** Same as **A** for a resistance altering sporulation rate (TSR scenario). **C** Basic reproduction numbers of the pathogen phenotype values μ_R (specialist, $\rho_{S,R} > 1$) and μ_G (generalist, $\rho_{S,R} < 1$). **D** Difference between the basic reproduction numbers of the pathogen phenotype values μ_R and μ_S. **E** Epidemiological protection for the TIE scenario as measured by the relative HAD. **F** Same as **E** for the TSR scenario.

B Properties of the mutation kernel m_ε

The kernel function m_ε arising in (2.1) should satisfy the following properties:

(H1) It should be non-negative everywhere: $m_\varepsilon = m_\varepsilon(x) \geq 0, \quad \forall x \in \mathbb{R}^N$. Moreover, m_ε should be normalised,

$$\int_{\mathbb{R}^N} m_\varepsilon(x)\mathrm{d}x = 1.$$

This last condition expresses that all interactions generated on the phenotypic space of pathogens necessarily end up somewhere on that space.

(H2) Its variation should only depend on the distance separating the points between which the interactions are evaluated (*i.e.* $m_\varepsilon(x) = m_\varepsilon(-x)$, for all $x \in \mathbb{R}^N$).

(H3) It is highly concentrated such that, for $\varepsilon \to 0$, $m_\varepsilon(x) = \delta_0(x) = 1$ if $x = 0$; and 0 otherwise.

C Some special cases of the general model (2.1)

We consider a slightly simplified version of system (2.1) by omitting the age structure. In that context we re-write model (2.1) as follows

$$\begin{cases} \partial_t S_k(t) = \varphi_k \Lambda - \theta S_k(t) - S_k(t) \displaystyle\int_{\mathbb{R}^N} \beta_k(y) A_k(t,y)\mathrm{d}y, \\ \partial_t I_k(t,x) = \beta_k(x) S_k(t) A(t,x) - \left(\theta + d_k(x) + \dfrac{1}{l_k(x)}\right) I_k(t,x), \\ \partial_t A(t,x) = -\delta A(t,x) + \displaystyle\sum_{k=1}^{n_c} \int_{\mathbb{R}^N} m_\varepsilon(x-y) p_k(y) I_k(t,y)\mathrm{d}y, \end{cases} \tag{C.1}$$

wherein we take into account the (host and strain-specific) duration of the sporulation period, denoted by $l_k(x)$.

Furthermore, if we assume that there are no "interactions" in the phenotypic space of pathogens, *i.e.* without mutations: $\varepsilon \to 0$, then the simplified model (C.1) rewrites

$$\begin{cases} \partial_t S_k(t) = \varphi_k \Lambda - \theta S_k(t) - S_k(t) \displaystyle\int_{\mathbb{R}^N} \beta_k(y) A_k(t,y)\mathrm{d}y, \\ \partial_t I_k(t,x) = \beta_k(x) S_k(t) A(t,x) - \left(\theta + d_k(x) + \dfrac{1}{l_k(x)}\right) I_k(t,x), \\ \partial_t A(t,x) = \displaystyle\sum_{k=1}^{n_c} p_k(x) I_k(t,x) - \delta A(t,x). \end{cases} \tag{C.2}$$

D Computation of the fitness function

In this appendix we explain how to compute the fitness function. To that aim, by formally taking the limit $\varepsilon \to 0$ into (2.1), this system becomes

$$\begin{cases} \partial_t S_k(t) = \varphi_k \Lambda - \theta S_k(t) - S_k(t) \displaystyle\int_{\mathbb{R}^N} \beta_k(y) A(t,y) \mathrm{d}y, \\ (\partial_t + \partial_a)\, i_k(t,a,x) = -\left(\theta + d_k(a,x)\right) i_k(t,a,x), \\ i_k(t,0,x) = \beta_k(x) S_k(t) A(t,x), \\ \partial_t A(t,x) = \displaystyle\sum_{l=1}^{n_c} \int_0^\infty r_l(a,x) i_l(t,a,x) \mathrm{d}a - \delta A(t,x). \end{cases} \tag{D.3}$$

Now, let us assume that system (D.3) reaches a monomorphic epidemiological equilibrium $E^z = (S_k^z, i_k^z(\cdot)\delta_z, A^z\delta_z)_{k=1,\cdots n_c}$, for some trait z, before a new mutation with trait value, say, y occurs. Note that E^z is the environmental feedback of the resident z. We introduce a small perturbation in (D.3) in the phenotype trait y, so that the evolution of the system reads as follows: $S_k(t) = S_k^z + u_k(t)$ and

$$i_k(t,a,x) = i_k^z(a)\delta_z(x) + j_k(t,a)\delta_y(x) \text{ and } A(t,x) = A^z\delta_z(x) + B(t)\delta_y(x),$$

and the small perturbations for the infection, j_k and B, are governed by the linearized system of equations around E^z. This reads as

$$\begin{cases} (\partial_t + \partial_a)\, j_k(t,a) = -\left(\theta + d_k(a,y)\right) j_k(t,a), \\ j_k(t,0) = \beta_k(y) S_k^z B(t), \\ B'(t) = \displaystyle\sum_{l=1}^{n_c} \int_0^\infty r_l(a,y) j_l(t,a) \mathrm{d}a - \delta B(t). \end{cases} \tag{D.4}$$

In order to study the evolution of this perturbation we will derive a renewal equation on $b^z(t,y)$, the density of newly produced spores at time t with phenotype y in the resident population with phenotype x. This term is more precisely defined by

$$b^z(t,y) = \sum_{l=1}^{n_c} \int_0^\infty r_l(a,y) j_l(t,a) \mathrm{d}a.$$

It then follows from the j_k-equation of the linear system (D.4), that

$$j_k(t,a) = \begin{cases} j_k(0,a-t) e^{-\theta t - \int_{a-t}^a d_k(\sigma,y)\mathrm{d}\sigma}, & a \geq t \\ \beta_k(y) S_k^z B(t-a) e^{-\theta a - \int_0^a d_k(\sigma,y)\mathrm{d}\sigma}, & a < t, \end{cases}$$

while

$$B(t) = \int_0^t b^z(s,y) e^{-\delta(t-s)} \mathrm{d}s + B(0) e^{-\delta t}.$$

As a consequence, $b^z(t,y)$ satisfies the following renewal equation:

$$b^z(t,y) = \sum_{l=1}^{n_c} S_l^z \int_0^t r_l(a,y)\beta_l(y) \int_0^{t-a} b^z(s,y) e^{-\delta(t-a-s)} e^{-\theta a - \int_0^a d_k(\sigma,y)\mathrm{d}\sigma} \mathrm{d}s\mathrm{d}a + \mathcal{F}(t,y,z), \tag{D.5}$$

wherein we have set

$$\begin{aligned}\mathcal{F}(t,y,z) = &\sum_{l=1}^{n_c} \int_t^{\infty} r_l(a,y) j_l(0,a-t) e^{-\theta t - \int_{a-t}^a d_k(\sigma,y)\mathrm{d}\sigma} \mathrm{d}a \\ &+ B(0) \sum_{l=1}^{n_c} S_l^z \int_0^t r_l(a,y)\beta_l(y) e^{-\delta(t-a)} e^{-\theta a - \int_0^a d_k(\sigma,y)\mathrm{d}\sigma} \mathrm{d}a.\end{aligned}$$

Then (D.5) can be rewritten as

$$b^z(t,y) = \int_0^t B^z(a,y) b^z(t-a,y)\mathrm{d}a + \mathcal{F}(t,y,z),$$

where $B^z(a,y)$ is the expected number of new infections produced per unit time, in a resident host population with phenotype z, by an individual which was infected a units of time ago with the phenotype y, given by

$$B^z(a,y) = e^{-\delta a} \sum_{l=1}^{n_c} S_l^z \beta_l(y) \int_0^a r_l(s,y) e^{-\theta s - \int_0^s d_k(\sigma,y)\mathrm{d}\sigma} \mathrm{d}s.$$

Due to the above formulation, it follows from classical adaptive dynamics (Diekmann et *al.*, 2005; Geritz et *al.*, 1997; Metz et *al.*, 1996) that the spore numbers, $R(y,E^z)$, of a rare mutant strategy, y, in the resident z-population is given by

$$R(y,E^z) = \int_0^{\infty} B^z(a,y)\mathrm{d}a = \frac{\Lambda}{\theta} f_z(y),$$

where $f_z(y)$ denotes the growth rate of a mutant strategy, y, in the resident z-population defined by

$$f_z(y) = \sum_{l=1}^{n_c} \frac{\theta S_l^z}{\Lambda} \Psi_l(y)$$

wherein $\Psi_l(y) = \frac{1}{\delta}\beta_l(y) \int_0^{\infty} r_l(a,y) \exp\left(-\theta a - \int_0^a d_l(\sigma,y)\mathrm{d}\sigma\right) \mathrm{d}a$.

Note that when the environmental feedback E^z is reduced to the disease-free environment, then S_l^z re-writes as $S_l^z = \frac{\Lambda\varphi_l}{\theta}$. And the epidemiological basic reproduction number of the pathogen with the phenotype y is calculated as

$$R_0(y) = \frac{\Lambda}{\theta}\Psi(y), \text{ with } \Psi(y) = \sum_{l=1}^{n_c} \varphi_l \Psi_l(y).$$

Once the pathogen has spread and reached the monomorphic equilibrium, then the endemic feedback environment E^z becomes

$$S_k^z = \frac{\Lambda\varphi_k}{\theta + \beta_k(z)A^z}, \quad i_k^z(a) = \beta_k(z)A^z S_k^z \exp\left(-\theta a - \int_0^a d_k(\sigma, z)\mathrm{d}\sigma\right), \quad \text{(D.6)}$$

where $A^z > 0$ is the unique solution of the following equation (only defined when $\mathcal{R}_0(z) > 1$):

$$\sum_{k=1}^{n_c} \frac{\Lambda\varphi_l}{\theta + \beta_k(z)A^z}\Psi_k(z) = 1. \quad \text{(D.7)}$$

E Pathogen fitness with mutations in the phenotypic space

In the context of this work, the fitness function Ψ can be used as a measure of absolute fitness. Indeed, when infection efficiencies do not differ between host classes (i.e. $\beta_k(x) = \beta(x)\ \forall\ k$), the fitness proxy $\mathcal{R}(x, y)$ simply writes

$$\mathcal{R}(x, y) = \frac{\Lambda}{\theta + \beta(x)A^x}\Psi(y) = \frac{\Psi(y)}{\Psi(x)},$$

where the last equality $\mathcal{R}(x, y) = \Psi(y)/\Psi(x)$ is obtained from the equation (D.7). It follows that a rare mutant will invade the population if $\Psi(y) > \Psi(x)$ (or $\mathcal{R}_0(y) > \mathcal{R}_0(x)$), which means that we can use R_0 (or Ψ) as a measure of absolute fitness in this case.

Now, assume that the infection efficiency differ between host classes. To simplify the presentation, we consider the case of two host classes. Then

$$\mathcal{R}(x, y) = \frac{\Lambda\varphi_1\Psi_1(y)}{\theta + \beta_1(x)A^x} + \frac{\Lambda\varphi_2\Psi_2(y)}{\theta + \beta_2(x)A^x},$$

wherein A^x is defined by (D.7). A straightforward computation leads to

$$\begin{aligned}
\mathcal{R}(x, y)\frac{\Psi(x)}{\Psi(y)} &= \left[\frac{\Lambda\varphi_1\Psi_1(y)}{\theta + \beta_1(x)A^x} + \frac{\Lambda\varphi_2\Psi_2(y)}{\theta + \beta_2(x)A^x}\right] \times \frac{\varphi_1\Psi_1(x) + \varphi_2\Psi_2(x)}{\varphi_1\Psi_1(y) + \varphi_2\Psi_2(y)}, \\
&= \left[\frac{\varphi_1^2\Psi_1(y)\Psi_1(x)}{\theta + \beta_1(x)A^x} + \frac{\varphi_1\varphi_2\Psi_1(y)\Psi_2(x)}{\theta + \beta_1(x)A^x} + \frac{\varphi_1\varphi_2\Psi_2(y)\Psi_1(x)}{\theta + \beta_2(x)A^x} + \frac{\varphi_2^2\Psi_2(y)\Psi_2(x)}{\theta + \beta_2(x)A^x}\right] \\
&\quad \times \frac{\Lambda}{\varphi_1\Psi_1(y) + \varphi_2\Psi_2(y)}.
\end{aligned} \quad \text{(E.8)}$$

Because of a strong trade-off between host classes, the product $\Psi_1\Psi_2 \ll 1$ and (E.8) becomes

$$\begin{aligned}
\mathcal{R}(x, y)\frac{\Psi(x)}{\Psi(y)} &\approx \left[\frac{\varphi_1^2\Psi_1(y)\Psi_1(x)}{\theta + \beta_1(x)A^x} + \frac{\varphi_2^2\Psi_2(y)\Psi_2(x)}{\theta + \beta_2(x)A^x}\right] \times \frac{\Lambda}{\varphi_1\Psi_1(y) + \varphi_2\Psi_2(y)}, \\
&= \left[\varphi_1\Psi_1(y)\left(1 - \frac{\Lambda\varphi_2\Psi_2(x)}{\theta + \beta_1(x)A^x}\right) + \varphi_2\Psi_2(y)\left(1 - \frac{\Lambda\varphi_1\Psi_1(x)}{\theta + \beta_2(x)A^x}\right)\right] \frac{1}{\varphi_1\Psi_1(y) + \varphi_2\Psi_2(y)},
\end{aligned}$$

where the last equality comes from (D.7). Again, by neglecting the term $\Psi_1\Psi_2$ we find $\mathcal{R}(x,y)\frac{\Psi(x)}{\Psi(y)} \approx 1$, meaning that the invasion fitness $\mathcal{R}(x,y)$ can be approximated by the ratio $\Psi(y)/\Psi(x)$.

Next, we further take into account small mutations in the space of pathogen phenotypic values (characterized by a sufficiently small parameter $\varepsilon > 0$). Our aim is to calculate the effect of mutation on pathogen fitness.

More precisely, consider a specific pathogen strain with phenotypic value x^* such that the Hessian matrix $-\mathbb{H}[\Psi](x^*)$ of the fitness function Ψ at point x^* is positive definite, meaning that $\Psi(x^*)$ is a global fitness peak. Then, from results in Djidjou-Demasse et *al.* (2017), the fitness of the pathogen strain x^* is expanded as

$$\Psi^\varepsilon(x^*) = \Psi(x^*)\left(1 - \varepsilon\frac{\mathrm{tr}\left[-K^*\right]^{\frac{1}{2}}}{2\sqrt{\Psi(x^*)}}\right) + o(\varepsilon), \tag{E.9}$$

wherein $\mathrm{tr}(\cdot)$ is set for the trace of a matrix (the sum of the elements on the main diagonal). $K^* = (k_{i,j})_{i,j}$ is a $N\times N$ matrix such that $k_{i,j} = (\delta_{i,l})_{1\le i\le N}^T \Sigma[m]^{-1} (\delta_{l,j})_{1\le i\le N} \frac{\partial^2\Psi(x^*)}{\partial_{x_i}\partial_{x_j}}$, where $\Sigma[m] = (\Sigma_{i,j})_{i,j}$ is the covariance matrix of the mutation kernel m defined by $\Sigma_{i,j} = \int_{\mathbb{R}^N} y_i y_j m(y)\mathrm{d}y$, and $\delta_{i,j} = 1$ if $i = j$; 0 otherwise. Furthermore, when the phenotypic value x is a scalar parameter (*i.e.* $x \in \mathbb{R}$) (E.9) takes the form

$$\Psi^\varepsilon(x^*) = \Psi(x^*)\left(1 - \varepsilon\frac{\sqrt{-\Psi''(x^*)}}{2\sqrt{\Psi(x^*)}}\right) + o(\varepsilon). \tag{E.10}$$

F Dimorphic or monomorphic equilibrium

To simplify the presentation, we consider system (2.1) with $n_c = 2$ corresponding to S and R cultivars. Denote by $(S_0, i_0(\cdot), A_0)$ the endemic equilibrium of system (2.1) as $\varepsilon \to 0$ and when only S is cultivated (*i.e.* when the proportion φ of R is zero). From results in (Djidjou-Demasse et *al.*, 2017) we have

$$S_0 = \frac{1}{\Psi_S(\mu_S)}. \tag{F.11}$$

Now, let $(S_S, S_R, i_S(\cdot), i_R(\cdot), A)$ be an equilibrium of system (2.1) when a proportion $\varphi > 0$ of R is cultivated. Next recall that, for $k \in \{S, R\}$,

$$S_k = \frac{\varphi_k\Lambda}{\theta + \int_{\mathbb{R}^N}\beta_k(z)A(z)\mathrm{d}z} \text{ and } i_k(x,a) = \beta_k(x)A(x)S_k\exp\left(-\theta a - \int_0^a d_k(\sigma,x)\mathrm{d}\sigma\right),$$

so that $A(\cdot)$ becomes a solution of the nonlinear equation:

$$\int_{\mathbb{R}^N} m_\varepsilon(x-y)\sum_{k\in\{S,R\}}\frac{\varphi_k\Psi_k(y)}{\theta + \int_{\mathbb{R}^N}\beta_k(z)A(z)\mathrm{d}z}A(y)\mathrm{d}y = \frac{1}{\Lambda}A(x). \tag{F.12}$$

Using this equation we heuristically explore conditions yielding to dimorphic or monomorphic equilibrium.

Resistant gene altering infection efficiencies β_S and β_R (TIE scenario). We formally assume that the population of spores writes $A(x) = a_S\delta_{\mu_S}(x) + a_R\delta_{\mu_R}(x)$, and we plug this ansatz into equation (F.12) above. This yields, for any x,

$$\begin{aligned}
&a_R\left[\frac{\varphi\Psi_R(\mu_R)}{\theta + a_R\beta_R(\mu_R) + a_S\beta_R(\mu_S)} + \frac{(1-\varphi)\Psi_S(\mu_R)}{\theta + a_R\beta_S(\mu_R) + a_S\beta_S(\mu_S)}\right] m_\varepsilon(x-\mu_R)\\
&+ a_S\left[\frac{\varphi\Psi_R(\mu_S)}{\theta + a_R\beta_R(\mu_R) + a_S\beta_R(\mu_S)} + \frac{(1-\varphi)\Psi_S(\mu_S)}{\theta + a_R\beta_S(\mu_R) + a_S\beta_S(\mu_S)}\right] m_\varepsilon(x-\mu_S)\\
&= \frac{1}{\Lambda}\left[a_R\delta_{\mu_R}(x) + a_S\delta_{\mu_S}(x)\right].
\end{aligned}$$

Letting $\varepsilon \to 0$ and recalling that $m_\varepsilon(x) \approx \delta_0(x)$, one obtains

$$\begin{aligned}
&a_R\left[\frac{\varphi\Psi_R(\mu_R)}{\theta + a_R\beta_R(\mu_R) + a_S\beta_R(\mu_S)} + \frac{(1-\varphi)\Psi_S(\mu_R)}{\theta + a_R\beta_S(\mu_R) + a_S\beta_S(\mu_S)}\right] \delta_{\mu_R}(x)\\
&+ a_S\left[\frac{\varphi\Psi_R(\mu_S)}{\theta + a_R\beta_R(\mu_R) + a_S\beta_R(\mu_S)} + \frac{(1-\varphi)\Psi_S(\mu_S)}{\theta + a_R\beta_S(\mu_R) + a_S\beta_S(\mu_S)}\right] \delta_{\mu_S}(x)\\
&= \frac{1}{\Lambda}\left[a_R\delta_{\mu_R}(x) + a_S\delta_{\mu_S}(x)\right],
\end{aligned}$$

that is

$$\begin{cases}
\dfrac{a_R\varphi\Psi_R(\mu_R)}{\theta + a_R\beta_R(\mu_R) + a_S\beta_R(\mu_S)} + \dfrac{a_R(1-\varphi)\Psi_S(\mu_R)}{\theta + a_R\beta_S(\mu_R) + a_S\beta_S(\mu_S)} = \dfrac{a_R}{\Lambda},\\
\dfrac{a_S\varphi\Psi_R(\mu_S)}{\theta + a_R\beta_R(\mu_R) + a_S\beta_R(\mu_S)} + \dfrac{a_S(1-\varphi)\Psi_S(\mu_S)}{\theta + a_R\beta_S(\mu_R) + a_S\beta_S(\mu_S)} = \dfrac{a_S}{\Lambda}.
\end{cases}$$

As a consequence, for the equilibrium to be dimorphic, namely $a_R > 0$ and $a_S > 0$, it is necessary that there exist $a_R > 0$ and $a_S > 0$ satisfying the following system of equations:

$$\begin{cases}
\dfrac{\varphi\Psi_R(\mu_R)}{\theta + a_R\beta_R(\mu_R) + a_S\beta_R(\mu_S)} + \dfrac{(1-\varphi)\Psi_S(\mu_R)}{\theta + a_R\beta_S(\mu_R) + a_S\beta_S(\mu_S)} = \dfrac{1}{\Lambda},\\
\dfrac{\varphi\Psi_R(\mu_S)}{\theta + a_R\beta_R(\mu_R) + a_S\beta_R(\mu_S)} + \dfrac{(1-\varphi)\Psi_S(\mu_S)}{\theta + a_R\beta_S(\mu_R) + a_S\beta_S(\mu_S)} = \dfrac{1}{\Lambda}.
\end{cases}$$

We suspect that this heuristic condition is a necessary and sufficient for system (2.1) (here with $n_c = 2$) to admit an endemic dimorphic equilibrium. This issue will be rigorously investigated in a forthcoming work.

In order to go slightly further in this analysis, we assume a strong trade-off on infection efficiency, namely

$$\Psi_l(\mu_k) < 1 \text{ and } \beta_l(\mu_k) \ll 1 \text{ for } l, k = R, S \text{ and } l \neq k.$$

In that the above system of equation roughly simplifies into

$$\begin{cases}
\dfrac{\varphi\Psi_R(\mu_R)}{\theta + a_R\beta_R(\mu_R)} \approx \dfrac{1}{\Lambda},\\
\dfrac{(1-\varphi)\Psi_S(\mu_S)}{\theta + a_S\beta_S(\mu_S)} \approx \dfrac{1}{\Lambda}.
\end{cases}$$

Hence the proportions of each phenotype, μ_S and μ_R, can be calculated as

$$a_R \approx \frac{\varphi\Lambda\Psi_R(\mu_R) - \theta}{\beta_R(\mu_R)} \quad \text{and} \quad a_S \approx \frac{(1-\varphi)\Lambda\Psi_S(\mu_S) - \theta}{\beta_S(\mu_S)}, \tag{F.13}$$

provided the following threshold conditions in this strong trade-off framework

$$\varphi\frac{\Lambda}{\theta}\Psi_R(\mu_R) > 1 \text{ and } (1-\varphi)\frac{\Lambda}{\theta}\Psi_S(\mu_S) > 1.$$

As a consequence, the density of healthy hosts at equilibrium, when a proportion $\varphi > 0$ of R is cultivated, writes

$$S_S \approx \frac{1}{\Psi_S(\mu_S)} \quad \text{and} \quad S_R \approx \frac{1}{\Psi_R(\mu_R)}. \tag{F.14}$$

Therefore, (F.11)-(F.14) lead to $S_S + S_R = (1/\Psi_S(\mu_S) + 1/\Psi_R(\mu_R)) > S_0 = 1/\Psi_S(\mu_S)$ meaning that with a strong-trade off on infection efficiency, the time during which a proportion $\varphi > 0$ of R gene deployed remains beneficial (in terms of Healthy Area Duration gain) can be considered larger as possible.

Resistant gene altering sporulation rates p_S and p_R (TSR scenario). In this case, using the same argument as in (Djidjou-Demasse et *al.*, 2017) we can prove that the spore population is monomorphic at equilibrium such that $A(x) = a^*\delta_{\mu^*}(x)$; with $a^* > 0$, providing that we are not in a strict symmetric configuration of the fitness function. Moreover, with a strong trade-off on sporulation rate, it's well known that $\mu^* \in \{\mu_S, \mu_R\}$. Then, applying the same arguments as in the previous section lead to

$$\frac{a^*}{\theta + a^*\beta(\mu^*)} m_\varepsilon(x-\mu^*)\Psi(\mu^*) = \frac{a^*}{\Lambda}\delta_{\mu^*}(x).$$

Again with $\varepsilon \to 0$, it comes

$$a^* = \frac{\Lambda\Psi(\mu^*) - \theta}{\beta(\mu^*)} = \frac{\theta}{\beta(\mu^*)}\left[R_0(\mu^*) - 1\right],$$

with $R_0(\mu^*) > 1$.

Therefore, the density of healthy hosts at equilibrium, when a proportion $\varphi > 0$ of R is cultivated, writes

$$S_S = \frac{1-\varphi}{\Psi(\mu^*)} \quad \text{and} \quad S_R = \frac{\varphi}{\Psi(\mu^*)}. \tag{F.15}$$

Therefore, (F.11)-(F.15) lead to $S_S + S_R > S_0$ if and only if $\Psi(\mu^*) < \Psi_S(\mu_S)$ meaning that with a strong-trade off on infection efficiency: (i) if $\Psi(\mu^*) < \Psi_S(\mu_S)$ the time during which a proportion $\varphi > 0$ of R gene deployed remains beneficial (in terms of Healthy Area Duration gain) can be consider larger as possible; (ii) else, this time is quantified by the unique time T such that $S_S(t) + S_R(t) \geq S_0(t)$ for all $0 < t \leq T$.